# BONE-PROSTHESIS INTERFACE RELATIVE DISPLACEMENT OF THE KNEE TIBIAL COMPONENT: FINITE ELEMENT ANALYSIS AND MEASUREMENT

by

H. Eskandari

A thesis submitted to the

Faculty of Graduate Studies and Research
in partial fulfilment of the requirements for the

Degree of Master of Engineering

Department of Mechanical Engineering

McGill University

Montreal, Quebec

July, 1993

Copyright © 1993, H. Eskandari

# INTERFACE RELATIVE DISPLACEMENT OF TIBIAL COMPONENT: FEA & MEASUREMENT

#### **ABSTRACT**

Despite significant improvements in total knee replacement surgery, loosening of the tibial prosthesis remains a major cause of failure of the procedure. Because of the limited fatigue life of the earlier fixation method which used PMMA as a bonding cement, biological fixation obtained by growth of bone into porous surfaces of the replacement prosthesis has become an attractive alternative. It is well established that bone ingrowth is strongly dependent on the relative displacement at the bone-prosthesis interface. Therefore, adequate immediate fixation is required to achieve durable biological fixation. In the absence of bonding cement, screws and press-fitted pegs are commonly used for initial fixation. The comparison of performance of these two methods in reducing relative displacement at the tibial prosthesis through both numerical and experimental approaches is the focus of this study.

A three dimensional finite element model of the resurfaced tibia was developed and analyzed using the finite element formulation of "contact" implemented in the ADINA software. The frictional effect at the interface was also included in the model. Two types of fixation strategy were modelled, the press-fit and screw fixation. The press-fit was modelled by overlapping the bone elements into the peg elements at the peg-hole interface. The screw fixation was modelled based on the effect of the tightened screw in introducing initial compressive force at the bone-prosthesis interface.

A photomicrographical technique linked with a video digitizing and image processing system were used to measure the relative displacement at the tibia-prosthesis interface. The measurements were performed for both screw and press-fit fixations.

Both the finite element analyses and measurements reveal that first, the interface relative displacements obtained by the two methods are in the same order of magnitude; second, the screw fixation significantly reduces the interface relative displacements in comparison with press-fit fixation.

#### RÉSUMÉ

Malgré d'importantes améliorations apportées à la chirurgie du remplacement du genou, la perte de la composante du tibia reste une des causes majeures de l'échec de l'opération. À cause des problèmes de fatigue écourtant la durée de vie de la fixation de la prothèse par ciment PMMA, la fixation biologique grâce à l'accroissement de l'os dans ces pores de la surface de la prothèse devient une alternative intéressante. Il est bien connu que cet accroissement de l'os est intimement relié au déplacement relatif à l'interface de l'os et de la prothèse. Par conséquent, il est essentiel d'avoir une fixation initiale immédiatement après l'opération chirurgicale afin de garantir une plus grande réussite de la fixation biologique. En alternative au ciment, les vis et les fiches entées serrées sont couramment utilisées pour la fixation initiale. La présente étude a pour but de comparer numériquement et expérimentalement la capacité de ces deux dernières méthodes à réduire le déplacement relatif à l'interface de l'os et de la prothèse.

Un modèle tridimensionnel d'éléments finis du tibia recouvert a été développé et analysé à l'aide de la formulation par éléments finis du "contact" implantée dans le programme commercial ADINA. L'effet de la fixation à l'interface est aussi considéré dans le modèle. Deux types de fixations sont étudiés: la fixation entré serré et la fixation par vis. La fixation entré serré était représentée en recouvrant les éléments de l'os par ceux de la fiche à leur interface commune, alors que la fixation par vis était représentée par la force compressive générée par serrage de la vis et exercée à l'interface de l'os et de la prothèse.

Une technique photomicrographique reliée à un magnétoscope numérique et à un système de traitement d'images était utilise afin de mesurer le déplacement relatif à l'interface du tibia et de la prothèse. Les mesures expérimentales étaient effectuées pour les fixations par vis et entré serré.

Les résultats obtenus par éléments finis et par mesures expérimentales révèlent en un premier temps que les déplacements relatifs à l'interface sont du même ordre de grandeur par l'une ou l'autre des méthodes et en un deuxième temps, que la fixation par vis réduit significativement les déplacements relatifs à l'interface de l'os et de la prothèse par rapport à la fixation entré serré.

#### **ACKNOWLEDGEMENT**

I wish to express my appreciation and gratitude to:

Professor A.M. Ahmed for his guidance and patience throughout this research,

Mustapha Tissakht, Neil Duncan, and Christopher McLean for various discussion and suggestions during the course of the research,

Wadood Hamad for reviewing this manuscript,

Arthur Clement and Tony Miccozi of the Machine Tool Laboratory for their help in the fabrication of prostheses required for the experiment.

#### **CONTENTS**

AB	STRACT	i	
AC	ACKNOWLEDGEMENTS		
LIS	T OF FIGURES	vi	
LIS	T OF TABLES	viii	
CHAPTER 1			
INT	RODUCTION	1	
1.1	General introduction	1	
1.2	Previous studies on evaluation of relative displacement		
	of the tibial prosthesis	2	
1.3	Present study and its objectives	7	
1.4	Organization of the thesis	7	
CHAPTER 2			
BIO	MECHANICS OF THE KNEE JOINT	9	
2.1	Introduction	9	
2.2	Anatomy of the knee joint	9	
2.3	Mechanics of the knee joint	11	
CHAPTER 3			
FIN	TE ELEMENT METHOD	16	
3.1	Introduction	16	
3.2	Finite element formulation of the contact problem	17	
3.3	Finite element model description	24	
3.4	Press-fit and screw fixation modelling	37	

#### CHAPTER 4 43 FINITE ELEMENT RESULTS 43 4.1 Introduction 43 Verification of results 4.2 Interpretation of results 46 4.3 CHAPTER 5 EXPERIMENTAL METHOD AND RESULTS 64 64 5.1 Introduction General test approach 5.2 65 65 5.3 Description of equipment Experimental method 71 5.4 74 5.5 Results CHAPTER 6 84 **DISCUSSION OF RESULTS** 84 6.1 Limitations of the study Comparison of finite element and experimental results 88 6.2 6.3 Comparison with previous studies 92 93 Clinical implications 6.4 CHAPTER 7 94 SUMMARY OF CONCLUSIONS 94 7.1 Introduction 94 Summary of conclusions 7.2 96 7.3 Directions for further studies

REFERENCES

97

#### LIST OF FIGURES

2.1	The knee joint, posterior view.	10
2.2	The bones of the leg, posterior view.	12
2.3	Forces on the lower leg during mid stance.	14
3.1	Contact in structures.	18
3.2	Gap element parameters.	19
3.3	Contact conditions using gap elements.	20
3.4	Schematic representation of contact conditions.	21
3.5	The 3-D finite element mesh of the prosthesis.	27
3.6	The 3-D finite element mesh of the tibia.	27
3.7	Distribution of elastic moduli of cancellous bone.	31
3.8	Distribution of elastic moduli of cortical bone.	33
3.9	Loading and boundary conditions.	34
3.10	Different arrangements of contactor and target surfaces.	36
3.11	The effect of bone radius on the pressure at the interface.	38
3.12	Initial displacement due to press-fit.	40
4.1	Contact forces at interfaces.	45
4.2	Load-displacement relation for the bone-prosthesis interface.	47
4.3	Effect of friction on the relative displacement at the	
	bone-prosthesis interface.	48
4.4	Displacements and relative displacements at the horizontal	
	interface for the close-fit model without friction.	50
4.5	Displacements and relative displacements at the horizontal	
	interface for the close-fit model with friction.	52
4.6	Displacements and relative displacements at the horizontal	
	interface for the press-fit model.	53
4.7	Comparison of relative displacements at the horizontal interface	

	for the close-fit and the press-fit models.	55
4.8	Comparison of relative displacements at the peg-hole interface	
	for the close-fit and the press-fit models.	55
4.9	Comparison of contact forces at the horizontal interface for	
	the close-fit and the press-fit models.	56
4.10	Contact pressures at the peg-hole interface due to press-fit.	58
4.11	Displacements and relative displacements at the horizontal	
	interface for the screw fixation model.	<b>5</b> 9
4.12	Comparison of relative displacements at the horizontal interface	
	for the close-fit and the screw fixation models.	60
4.13	Displacements of nodes along the tibial axis.	62
5.1	Experimental set-up.	66
5.2	Loading device.	67
5.3	A typical tibial specimen prepared for implantation.	73
5.4	Photomicrographic images of a typical location at the horizontal	
	interface before and after load application.	75
5.5	Pictorial representation of the sign convention used	
	in presenting the results.	76
5.6	Typical results of three separate measurements of interface	
	relative displacement in x-direction for one specimen with	
	pegged prosthesis.	77
5.7	Comparison of the finite element results of the interface relative	
	displacement and measurements for the press-fit fixation.	80
5.8	Comparison of the finite element results of the interface relative	
	displacement and measurements for the screw fixation.	82
5.9	Comparison of experimental results for the press-fit and the	
	screw fixations.	83
6.1	Comparison of finite element results for the press-fit and the	
	close-fit models and measurements for pegged prosthesis.	91

#### LIST OF TABLES

3.1	The elastic moduli of cancellous bone.	32
3.2	The elastic moduli of cortical bone.	33

# CHAPTER 1

#### INTRODUCTION

#### 1.1 GENERAL INTRODUCTION

Arthritis, a disease affecting the articular surfaces of synovial joints, is suffered by a significant proportion of the population. A common treatment for severe cases of arthritis is total joint arthroplasty, in which the affected surfaces of the joint are replaced by prosthetic components. For the knee, total knee arthroplasty (TKA) has succeeded not only in eliminating pain in patients but also in the restoration of mobility and load transmission at the joint. However, due to certain long term complications, this treatment requires further improvements. Loosening of prosthetic components is one of the complications yet to be resolved satisfactorily. Loosening, especially of the tibial prosthesis, has been one of the major causes of mechanical failure in total knee replacement. Therefore, fixation of this prosthesis to its surrounding bone remains a matter of continuing concern.

Prosthetic components may be fixed in place by mechanical or biological means. Early fixation methods used PMMA (polymethylmethacrylate) as a bonding cement to attach prostheses to bone. The method of using PMMA has been very successful in providing stable initial fixation by immediate polymerization of the cement. But its longevity has always been limited by the finite fatigue life of the bone-cement and of the cement-prosthesis interface. This limitation has motivated investigators to search for

alternative fixation methods.

Among the alternative methods, biological fixation, attained by growth of bone into the porous surface of a prosthesis, became an attractive alternative to cement fixation. At variance with cemented prosthesis with which an immediate fixation is achieved by the polymerization of the cement, a post-operative immobilization period or adequate initial fixation is needed for biological fixation to allow the bone ingrowth to occur.

Initial bone ingrowth into the porous surface of a prosthesis is known to be highly dependent on the relative displacement between the prosthesis and the host bone. Based on experimental results, it is believed that beyond a certain limit of relative displacement, only fibrous tissues will grow at the bone-prosthesis interface, resulting in a low-strength fixation. In order to obtain a high-strength fixation by bone ingrowth, adequate immediate fixation is required. The design of the prosthesis and the immediate fixation method requires understanding of the relation between the relative displacement at the interface and various parameters associated with the design of fixation. Towards this objective, researchers have employed both numerical and experimental methods.

### 1.2 PREVIOUS STUDIES ON EVALUATION OF RELATIVE DISPLACEMENT OF THE TIBIAL PROSTHESIS

As already mentioned, two approaches for the evaluation of the relative displacement at bone-prosthesis interfaces have been followed by previous researchers: the numerical and experimental approaches. The review of the literature begins with the finite-element-based researches, followed by the experimental studies.

#### FINITE-ELEMENT-BASED RESEARCHES

Finite element technique was first introduced to orthopaedic research in 1972. It was used to investigate the relationship between bone architecture and its load bearing function including the bone remodelling process, to evaluate and optimize artificial joints and fracture fixation devices, and to study the mechanical behaviour of soft tissues. A

survey of finite element based orthopaedic research, since the introduction of the finite element method to this field until 1982, is reported by Huiskes and Chao [1].

Recent advancements in finite element techniques have made it possible to use this tool for complex problems such as analysis of contact at natural or artificial joints. The finite element formulations of contact characteristics have been used by biomechanics researchers to evaluate relative displacement at the bone-prosthesis interfaces. Natarajan et al. [2] studied the effect of differences in the material properties of bone and prosthesis on relative displacement at the tibia-prosthesis interface using an axisymmetric finite element model. They modelled the interface by employing link elements with shear and normal stiffnesses. The shear stiffness was assigned to link elements to represent the friction at the interface. Their results showed that friction at the interface does not appear sufficient to prevent relative movement. The frictional parameter (i.e. shear stiffness) was varied through several orders of magnitude without changing the character of the results. They also concluded that elasticity differences of bone and prosthesis are likely to be a factor influencing bone ingrowth in the tibial prosthesis. In their later work [3] on the evaluation of relative displacement, they investigated the effect of different models of the cancellous bone structure on the prediction of relative displacement at the interface. Cancellous bone was modelled both as a continuum and as a lattice beam structure. In the latter model, the trabecular architecture was assumed to consist of a lattice of thin beams of specific density. They found that relative displacement is predicted to be higher when the cancellous bone is modelled as a lattice beam structure. Shirazi-Adl and Ahmed [4] did a parametric, axisymmetric study on the relative displacement of the boneprosthesis interface of a porous-surfaced tibial prosthesis. They also modelled interface condition by link elements and with only normal stiffness. They investigated the effect of various parameters such as contact spacing, height of a central stem, properties of the prosthesis and of the cortical shell, presence of UHMWP (ultra high molecular weight polyethylene) articular plate and the presence of a circumferential flange. The boneprosthesis interface was assumed to be frictionless, transferring only forces normal to the interface through link elements at the points of contact. In order to allow for separation

normal to the interface, those elements which resisted tensile stresses were discarded at the end of each iteration. They found that reduction in the height of the metal central stem has a negligible effect on the magnitude of the maximum displacements at the horizontal interface. Replacing Cobalt-Chromium metal alloy by titanium was found to result in an increase in displacements on both interfaces. The variation in the link spacing was predicted to have a negligible effect on the interface displacements.

Tissakht *et al.* [5] studied a three dimensional finite element model of a proximal tibia resurfaced by a two-pegged prosthesis. The contact conditions at the interface was modelled by link elements with normal stiffness. Their attempt was to validate finite element predictions with experimental measurements at corresponding coronal sections of the tibia. In these studies, static analysis was performed and material properties of bone were assumed to be linear, isotropic and inhomogeneous. Friction at the interface was not taken into account. Their results showed that the relative interface displacement is higher laterally and medially and decreases to a small value between the pegs. The measurements and finite element predictions exhibited the same variation along the bone-prosthesis interface; the magnitudes, however, were different.

As stated earlier, many finite element analyses were done in order to evaluate stress distribution at proximal tibia with or without prosthesis which are not referred to here. But one of these studies, despite its objective of stress determination, is related to the present study. Dawson *et al.* [6] have studied the effect of press-fit on the stresses at the peg-hole interface. Press-fit between the cancellous bone and the peg was represented by specifying an overlap of the bone elements relative to the peg elements.

Except for the study of Tissakht *et al.* [5], the other studies used only two dimensional or axisymmetric models. Due to the inadequately developed finite element formulation of contact characteristics, and also due to the absence of data on frictional properties between bone and prosthesis, friction was not taken into consideration in the above studies.

#### **EXPERIMENTAL STUDIES**

Most of the studies on the evaluation of relative displacement at interfaces of the tibial prosthesis have been conducted experimentally. Due to difficulties and limitations of in vivo studies, only few researches have been carried out in vivo [7,8]. The only available method which has been employed for in vivo studies is a radiographic method called Roentgen Stereogrammetric Analysis (RSA). Because of its low accuracy (0.2 mm, when applied to knee arthroplasty) it has not been used for in vitro studies. However, RSA has been used for the evaluation of relative displacement in vivo in terms of both migration (i.e., permanent relative displacement over time) and inducible displacement (i.e., recoverable displacement) [7,8].

Recoverable relative displacement (due to elastic deformation) has also been measured by more accurate methods. Several investigators have used Linear Variational Differential Transducer (LVDT) to measure the relative displacement between tibial prostheses and the tibia itself [9,10,11,12,13]. The accuracy of this measuring system is reported to be about  $\pm 2\mu m$  [10]. All these studies reported usage of LVDT mounted only at few locations.

Application of dial gauge for measuring relative displacement has been reported by others [14,15,16]. None of them has mentioned the accuracy of measurement. In some studies the method of conventional photomicrography, often linked with video digitizer, has been employed [5,17,18,19]. Yang *et al.* [19] reported the accuracy of their measuring device as  $7 \mu \text{m/pixel}$ .

Comparison of different fixation methods for their effect on reduction of relative displacement has been the objective of many studies. Miura et al. [15] studied the effect of application of screws on the relative displacement of the tibial prosthesis. Their results showed that the use of screws significantly reduced relative displacement. Rigid fixation was found to be achieved with screws even in specimens with low bone strength. The screws tended to override the effect of tight stem fixation. Sumner et al. [10] studied relative displacement of the tibial tray fixed with different combinations of pegs and screws. They concluded that the use of screws reduced the magnitudes of the initial

relative displacement. The relative displacements were not affected by the presence or the absence of pegs in prostheses which were held in place by screws. Strickland *et al.* [16] studied different fixation strategy using pegs, screws and stem. They found that the screw fixation of the tibial prosthesis is critical to the maintenance of initial stability of the prosthesis. Kaiser *et al.* [12] compared two fixation methods: a single, angled central peg and three peripheral screws. Their results suggested that the screw fixation is preferable in providing initial stability. The influences of the tibial tray surface types and the flexibility of prosthesis material on the relative displacement were studied by Yang *et al.* [19] and Yoshii *et al.* [9] respectively. Yang *et al.* studied two types of prosthesis surfaces: smooth and Ti fibre mesh. Their results showed that prostheses with fibre mesh surface had smaller relative displacements. The results of the study of Yoshii *et al.* suggested that tibial trays made with Ti provide more stable and rigid fixation when exposed to eccentric loading than Co-Cr trays.

Most of the studies have simulated the conditions of interface immediately after surgery [9,11,12,15,16,18,19]. In these tests, the prosthesis is inserted into cadaveric tibial specimens. Some studies have had experiments simulating the condition of interface several months after surgery [15,17]. In these experiments, a prosthesis is inserted into a tibia of an animal by surgery. After several months, the animal is sacrificed and the tibia is removed for tests.

Most of the above studies were concerned with the evaluation of the overall rigid body displacement of the prosthesis with respect to the bone, and only few [5,17,19] measured the local relative displacement at the bone-prosthesis interface. Yang et al.[19] reported the accuracy of their measuring system, and Tissakht et al. [5] compared their measurements with finite element predictions.

#### 1.3 PRESENT STUDY AND ITS OBJECTIVES

Finite element modelling of screw and press-fit fixations in order to predict relative displacement at the tibia-prosthesis interface and, comparison of these predictions with experimental results obtained from testing of similar fixations are the main objectives of this study.

Superior performance of screw fixation with respect to other types of fixation has been experimentally demonstrated in some previous studies [10,12,15,16]. But as yet no finite element model of screw fixation has been made. As a first attempt to the modelling of screw fixation, the effect of screws in the pre-loading of connected components is considered.

Due to limitations in the finite element code used by previous investigators, frictional properties at bone-prosthesis interface were not considered or were modelled in a rudimentary fashion. In this study, coefficient of friction is considered as an input to the finite element code.

An experimental study is also carried out to support finite element findings. Although the experimental method is not new, the equipment and technique of measurement are improved to gain higher accuracy in comparison to previous studies.

#### 1.4 ORGANIZATION OF THE THESIS

This research work deals with the evaluation of relative displacement of the tibial prosthesis in a resurfaced tibia of a human knee joint. Hence, first of all, Chapter 2 gives a basic account of the important characteristic of the knee joint and the terminology related to this study in order to provide an easier understanding of the succeeding chapters.

This study includes both experimental and theoretical approaches for the determination of relative displacement. Chapter 3 covers a brief description of the finite element formulation for contact problem. Details of mesh generation of the tibia and prosthesis and the description of the finite element models of screw and press-fit fixations are presented as well. The results of the finite element analysis and comments on their validation and interpretation are provided in Chapter 4.

Experimental preparation and procedure are described in Chapter 5. This chapter also covers a brief description of the measuring devices, their limitations and accuracy, and the results of the experimental measurements with pertinent commentary.

Chapter 6 provides a discussion of the comparison between the predictions of the finite element model and experimental results for the screw and press-fit fixations. Finally, the summary of conclusions of this work and directions for further studies are given in Chapter 7.

# CHAPTER 2

#### BIOMECHANICS OF THE KNEE JOINT

#### 2.1 INTRODUCTION

In order to familiarize the reader with the biomechanical aspects of this study, in this chapter general background information about the anatomy of the knee joint and its load transmission characteristics are provided.

In section two, a brief description of the anatomy of the knee joint is given. Since among the knee joint components, the tibia is the focus of this study, the anatomy of the tibia is described separately. However, additional information about the structure of the tibia can be found in Chapter 3.

In section three, the mechanics of the knee joint, particulary, the analysis of forces transmitted across the knee joint, are explained.

#### 2.2 ANATOMY OF THE KNEE JOINT

The knee joint consists of several parts: femur, tibia, patella (hard tissues), menisci, ligaments, capsule (soft tissues). There exist two articulations: One between the tibia and the femur (tibiofemoral) and the other between the patella and the femur (patellofemoral). In the tibiofemoral articulation the two condylar surfaces of the distal femur articulate with the two nearly flat surfaces of the tibial plateau. The two bones of

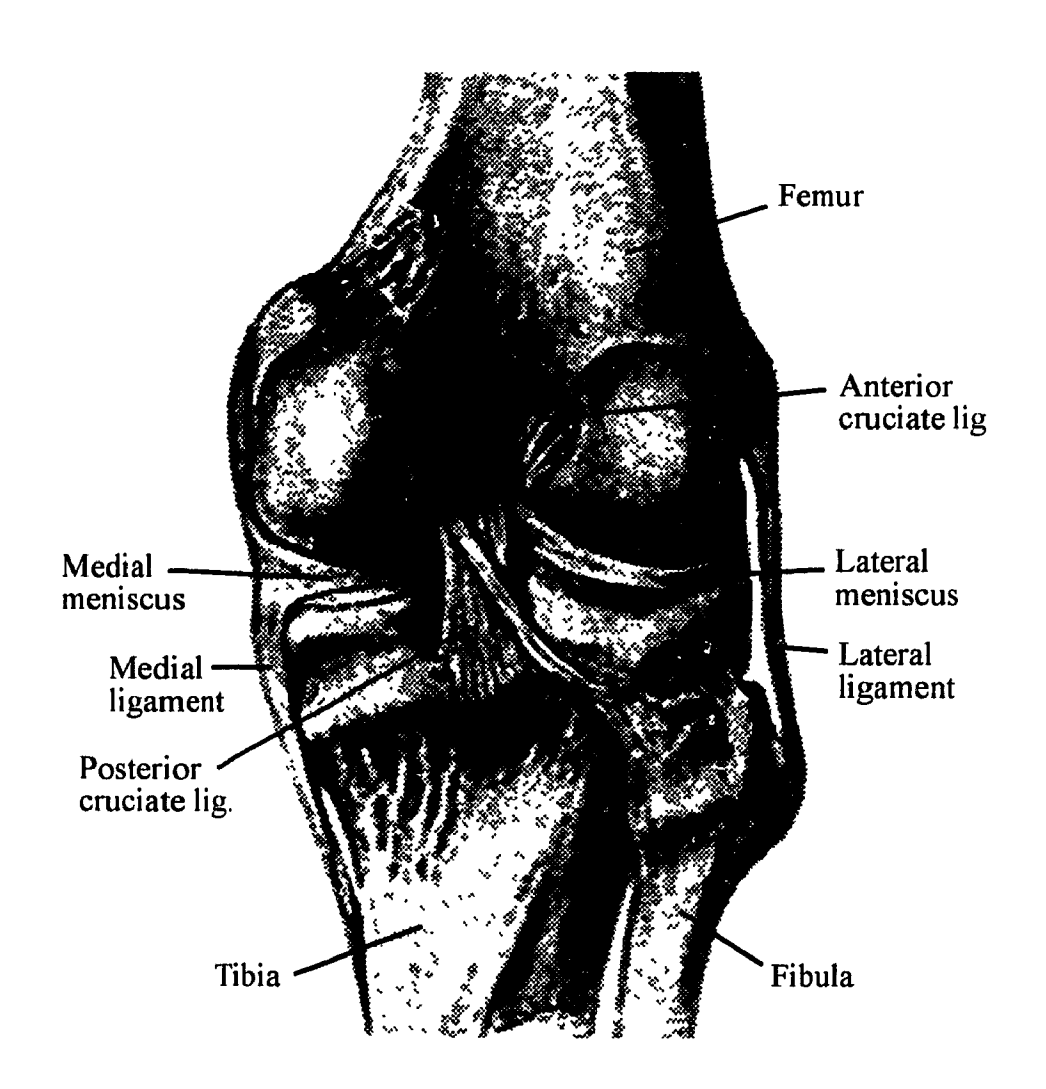


Fig. 2.1 The knee joint, posterior view [20]

10

this articulation are connected by four major- ligaments, the two collateral ones, one on each side, and the two cruciates in the central inter-condylar notch (see Fig. 2.1) [20]. The menisci are two crescentic pads each covering approximately two-thirds of the tibial plateau upon which they rest. One of the many functions of the menisci is that they serve to cushion the curved femoral condyles on the relatively flat tibial plateaus, increasing the congruency between them. The entire knee joint is covered by a thin, non-uniform, and strong fibrous Capsule.

#### ANATOMY OF THE TIBIA

The tibia is the second longest bone (after the femur) of the human skeleton. It articulates at its proximal end with the femur, and at its distal end with the talus of the ankle (see Fig. 2.2)

The tibia's upper extremity is large, and expanded into two eminences, the medial and lateral condyles, which are covered by articular cartilage. The central portions of these condyles articulate with the condyles of the femur, while their peripheral portions support the menisci of the knee joint. Between these articular facets is located the intercondyloid eminence. It has rough depressions for the attachment of the anterior and posterior cruciate ligaments and the menisci.

The body or shaft of the tibia spans between its two larger extremities. It has three surfaces which give attachment to numerous muscle groups.

The structure of the tibia is like that of the other long bones consisting of cancellous bone inside and cortical bone outside. The cortical wall is thickest at the junction of the middle and lower thirds of the bone. The cancellous bone is strongest immediately under the tibial condyles where it is called the subchondral bone. Detailed description of the mechanical properties of the bones of the tibia is given in Chapter 3.

#### 2.3 MECHANICS OF THE KNEE JOINT

In the animal skeleton, joints have two functions: to allow motion and to transmit load. The type of motion allowed by each joint varies according to the geometry of the

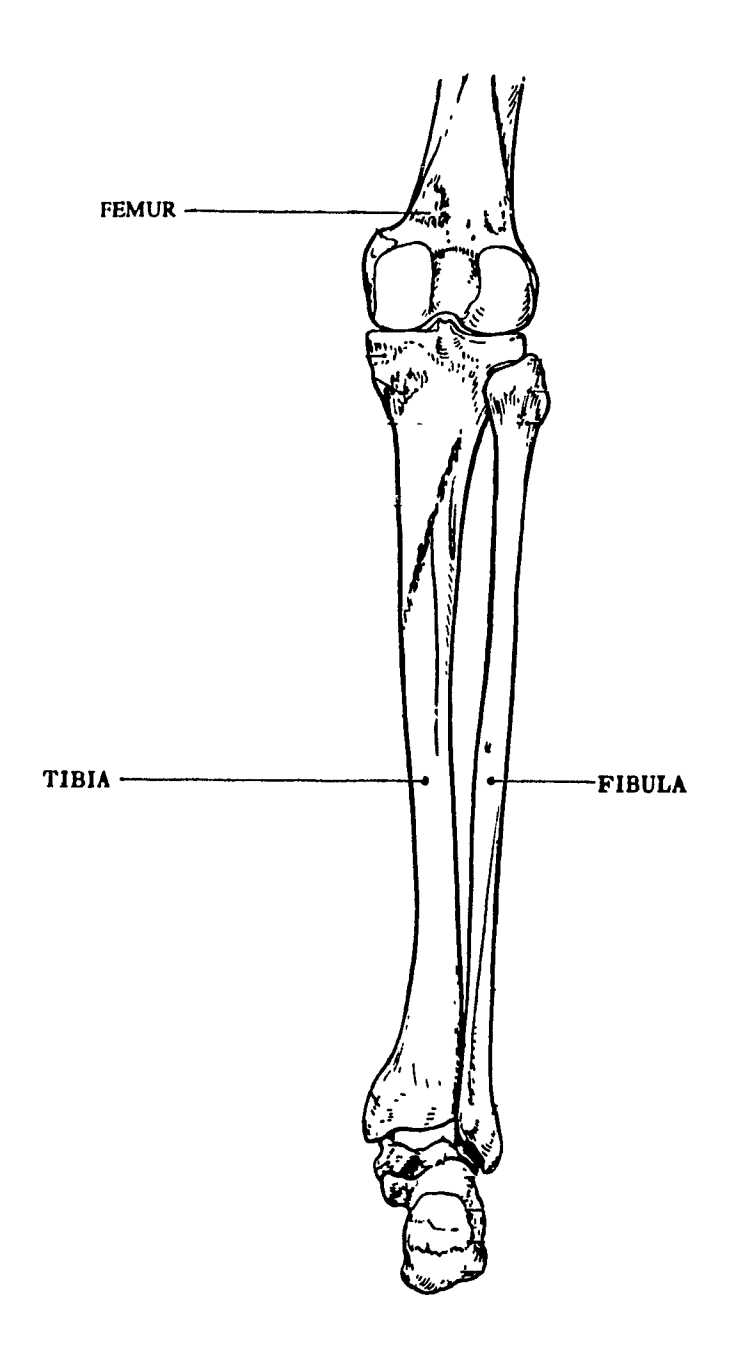


Fig. 2.2 The bones of the leg, posterior view [20].

joint surfaces and the nature of soft tissue constraints surrounding the joint. In general, joints can have one to three degrees of freedom for gross joint motion. The knee joint, for example, has its greatest range of motion in the movement of flexion and extension. Also the tibia rotates about an axis parallel to its long axis while going through the range of flexion and extension. In addition, if a varus or valgus moment is applied to the tibia, the knee can execute rotation about an anteroposterior axis. However, the knee joint is predominantly a single-degree-cf-freedom joint (flexion and extension) in contrast to the hip joint which has three degree-of-freedom. The motion at the joint articular surfaces is in the form of sliding and rolling.

The second function of a joint is to transmit loads. In the study of joint loads, three types of forces should be considered. These are: functional loads (gravity, Inertia, ground forces and other external forces), muscle forces, and joint forces.

Whenever a functional load is applied, there will be, in general, a muscle force produced to restrain the applied force. These two forces produce the joint-reaction forces: joint-contact force, and forces in the ligaments, menisci and the capsule [21]. However, the joint-contact force is usually the dominant force among the joint forces.

During the stance phase of gait, the force exerted against the foot is called the ground-reaction force (see Fig. 2.3) [22]. Ground-reaction forces during various activities have been measured by many investigators using a force-plate technique [23,24,25]. These forces vary from a maximum of 1.3 times body weight for normal walking to more than twice the body weight for running activities. The direction of this force is also variable during the gait cycle. Once the functional load has been established for a particular configuration of the limb, the muscle forces necessary to sustain this functional load can be calculated. The ground-reaction force in this particular phase of gait creates a moment about the knee joint, which tends to extend the knee. To resist this moment a hamstring force (muscle force) is required. Since the ground-reaction force has a moment arm (A) about the contact point of the knee joint that is much larger than the moment arm (B) for the hamstring force (M), the hamstring force will have to be much greater than the ground-reaction force to balance the moments about the contact point at

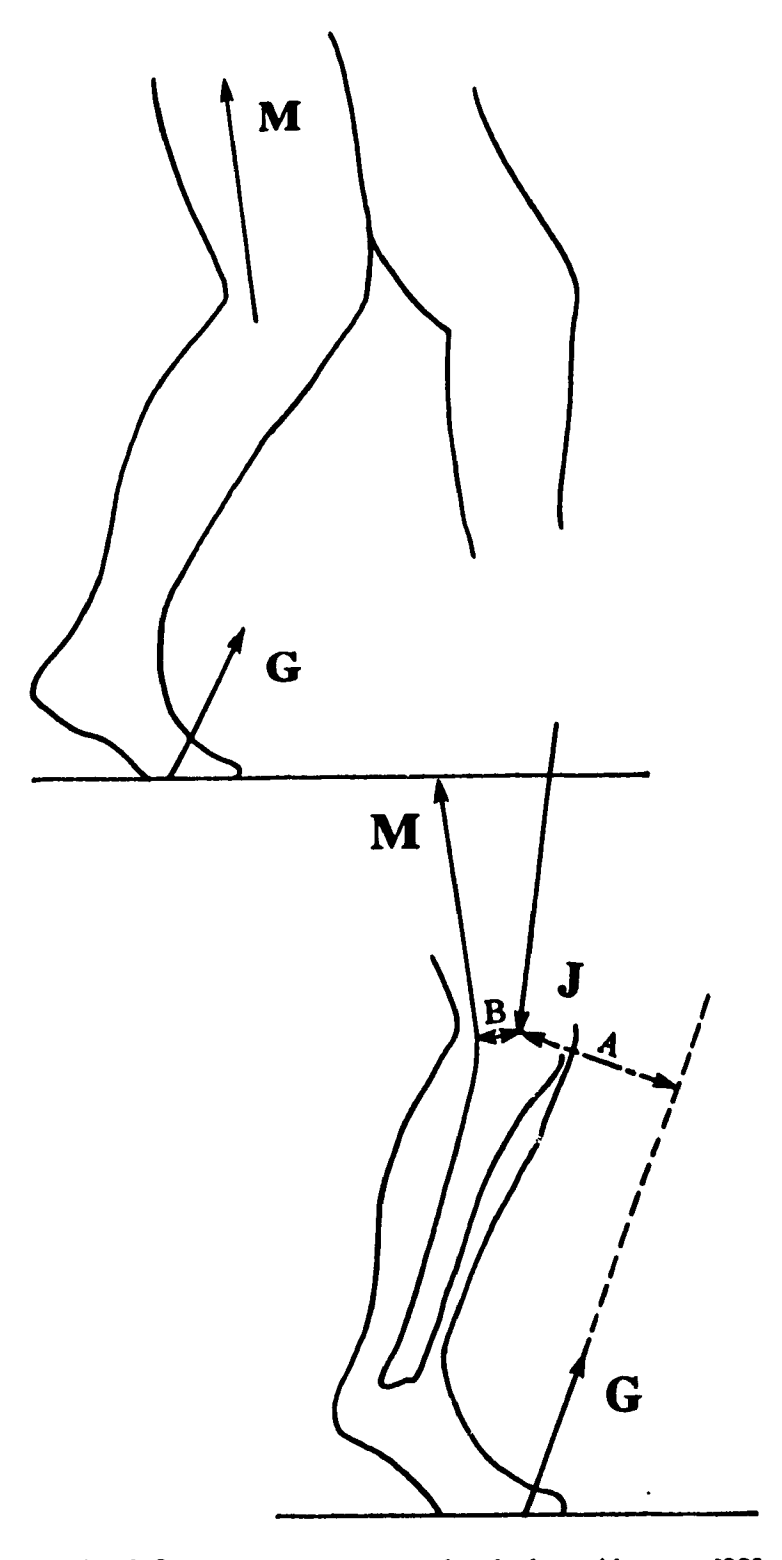


Fig. 2.3 Forces on the lower leg during mid stance [22];
M: Muscle force, G: Ground force, J: Joint force.

the knee joint. The major resultant of these two forces is the joint-contact force (J), which acts between the femur and tibia. This force is a result of the muscle force and the functional load and is controlled by the magnitude and direction of these two forces. Neglecting the other joint forces, the lower leg should be in equilibrium under the three dominant forces.

In general, the moment arm of the functional load can vary widely, but, the moment arm of the muscle forces are fixed by the anatomic positions of the muscles. Generally the ratio of moment arm of functional load to that of muscle force is somewhere between 1:1 to 6:1. As a result, the muscle force is several times larger than functional load. The joint-contact force is strongly related to the applied muscle force. Therefore, it is not surprising that several investigators [26,27] have shown that the joint-contact force ranges from two to seven times body weight for normal activities.

# CHAPTER 3

#### FINITE ELEMENT METHOD

#### 3.1 INTRODUCTION

A three dimensional finite element model of the proximal tibia resurfaced by a prosthesis was developed in order to evaluate the relative displacement at the tibia-prosthesis interface. The model was analyzed using the finite element formulation developed by Bathe *et al.* [28] for contact problems which is implemented in the commercially available ADINA (Automatic Dynamic Incremental Nonlinear Analysis) software package.

The model consists of two separate bodies, the tibia and the prosthesis, which are initially in close contact. The geometry of the tibial model was determined based on transverse CT-scan images of a tibia of average size. The finite element mesh was then generated using the FEMAP (Finite Element Modelling and Processing) pre-processor. A total of 1379 8-node brick and 6-node wedge elements and 1776 nodes were generated.

Cortical and cancellous bones were considered as linear, elastic, isotropic and inhomogeneous materials. Thirteen different elastic moduli were assigned to the different regions of the cancellous bone based on the data reported by Goldstein *et al.* [29]. The elastic modulus of the cortical bone, assumed to increase linearly from the proximal end to the distal end, was based on the data available in the literature [4,30,31]. Twelve different moduli of elasticity were assigned to the different levels of the cortical shell.

The conditions of two different fixation methods were modelled: press-fit and screw fixation. Press-fitting of the prosthesis into bone was modelled by overlapping the bone elements at the peg-hole interface into the peg elements. Screw fixation was modelled based on the effect of the tightened screw in introducing an initial compressive forces at the interface of the bone and prosthesis. Both models take into account frictional effects at interfaces.

In Section 3.2 of this chapter, the description of the finite element formulation of the contact problem is presented. The finite element model of the resurfaced tibia is described in Section 3.3 and, finally, the methods for the modelling of the press-fit and screw fixation are demonstrated in Section 3.4.

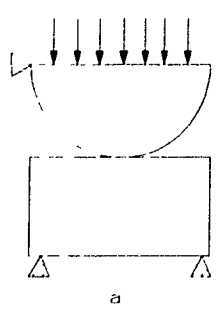
### 3.2 FINITE ELEMENT FORMULATION OF THE CONTACT PROBLEM NON-LINEAR FINITE ELEMENT ANALYSIS

Non-linear finite element analysis involves non-linear effects in structures or solid bodies which are due to various causes such as material plasticity, creep, non-linear elastic material properties and the presence of gaps in structures leading to contact. Methods of analysis of structures with gaps have been the subject of considerable research. Analytical solutions to particular contact problems with simple geometries do exist; however, analysis of structures with contact areas of complex geometry requires usage of finite element methods.

The main difference between linear and non-linear analyses, as far as the solution is concerned, is that the non-linear analysis requires several iterations to obtain a solution while the linear analysis yields a solution without iteration. This means that the CPU time of the computer or, in other words, the cost incurred in analyzing problems involving non-linear effects is much higher than for linear analysis.

#### MODELLING OF CONTACTS BY FINITE ELEMENT METHOD

In solid bodies or structures, contact occurs because of the interfacing of two or more objects or because of the closure of a gap in any one body (Fig. 3.1).



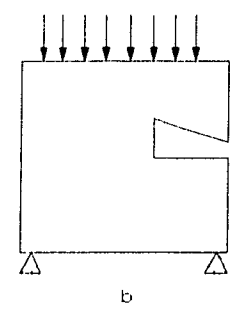


Fig. 3.1 Contact in structures.

- a) contact of two bodies (due to rigid body motion and/or deformation)
- b) contact in one body (due to deformation).

Despite the differences between these two cases, the basic problem is similar in that two points (or nodes) come into contact in response to the application of external loads and, consequently, normal and tangential forces are developed at the interface. Tangential forces are produced due to the frictional effect at the interface. It is evident that normal forces at the interface are compressive because tensile forces cannot be transferred across the interface.

Two methods are currently available for the solution of contact problems:

- Modelling with auxiliary elements: two-node elements are used at the interface which connect each two nodes that are in contact or are anticipated to come into contact.
- 2) Modelling without auxiliary elements: a more general formulation is used which is based on introducing contact surfaces.

#### 1) Modelling With Auxiliary Element

The contact between two nodes which belong to one or two different bodies can be modelled by using an element between the two nodes. The elements used for modelling interface conditions are referred to as link or gap or interface elements. These elements are two-node truss elements which connect two adjacent nodes that are in contact or are anticipated to come into contact. These elements are non-linear and considered to balance compressive load but not a tensile load. The frictional effect can

be formulated as well (e.g., as in MSC NASTRAN software).

In some formulations the length and cross sectional area and the modulus of elasticity of the material can be assigned to elements separately (e.g., ADINA software) and in some other formulations instead of these parameters, the stiffnesses of elements in axial and transverse directions can be used (e.g., MSC NASTRAN). In both cases, the stiffnesses of these elements are chosen to be close to that of the neighbouring grids. The stiffnesses considered for these elements can affect the convergence of the solution and even make the solution diverge.

The contact conditions are detected by applying certain criteria. These criteria are described below in the review of the formulation of gap elements.

In Fig. 3.2 w is the width of the gap (w  $\geq$  0),  $U_A$  and  $U_B$  are the displacements of the nodes A and B respectively, and  $\delta$  is the relative displacement of the nodes A and B ( $\delta = U_B - U_A$ ). Then the following criteria are defined:

- i) for  $\delta > 0$ , the stress in the truss is zero.
- ii) for  $\delta < 0$ , the effective strain ( $\epsilon_{\rm eff}$ ) used in the stress calculation is:  $\epsilon_{\rm eff} = 0.0 \quad \text{if} \quad |\delta| \leq w,$   $\epsilon_{\rm eff} = (\delta + w)/\ell \quad \text{if} \quad |\delta| > w; \quad \text{where } \ell \text{ is the length of the element.}$

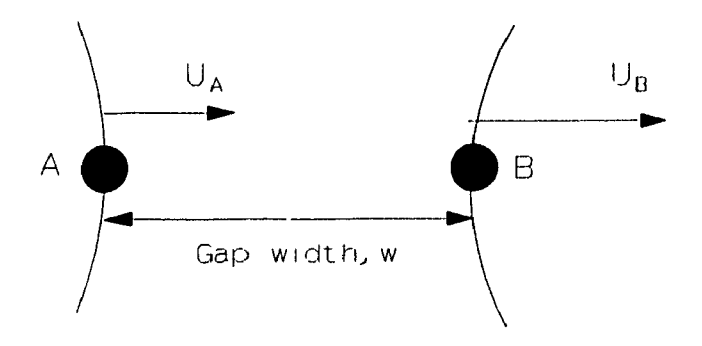


Fig. 3.2 Gap element parameters.

Some states of displacements of nodes which correspond to the above conditions are shown below.

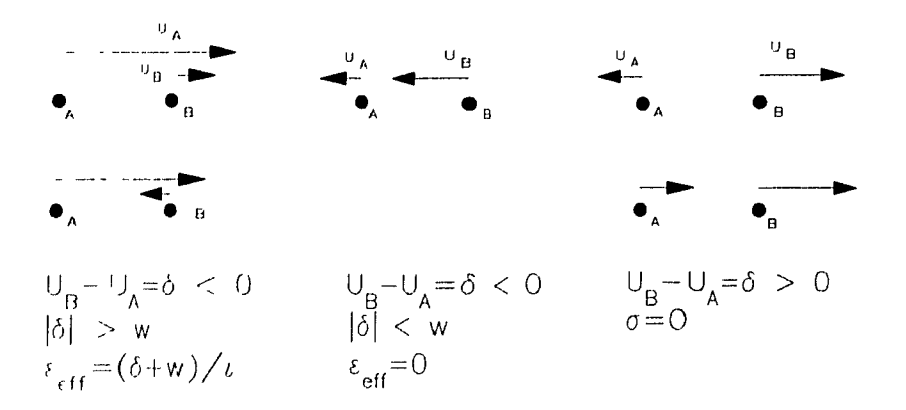


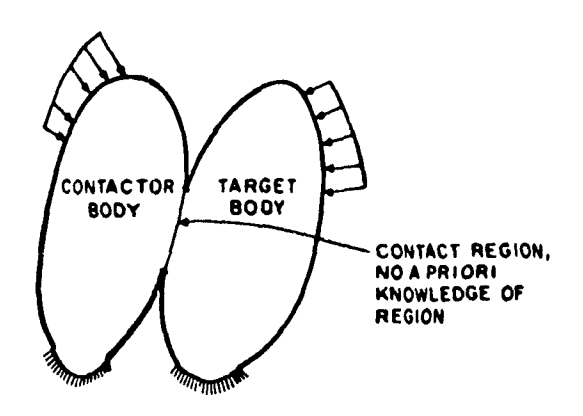
Fig. 3.3 Contact conditions using gap elements.

In the above formulation, the stress-strain relation will be defined by the material model of the element. With this formulation it is possible to introduce pre-stress at the interface which is useful for the modelling of the press-fit condition. In some formulations, these conditions are expressed based on force and displacement (e.g. MSC NASTRAN) instead of stress and strain. The MSC NASTRAN formulation also takes into account the frictional effect at the interface. Frictional forces are handled in this program by adding another condition to the above conditions which is:  $F_f = \mu F_x$ , if  $F_x$  is compressive; and  $F_f = 0$ , if  $F_x$  is tensile [32].

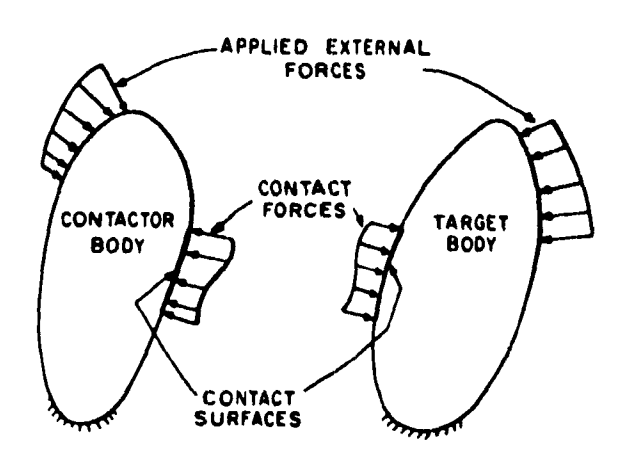
#### 2) Modelling Without Auxiliary Elements

In this method, contact surfaces are defined as regions of two or more bodies which are anticipated to come into contact. These bodies are denoted as the contactor and the target, and their associated contact surfaces are termed contactor and target surfaces respectively (Fig. 3.4).

The main concept in this method is that contact forces will develop along contact surfaces when bodies are in contact. These forces are equal and opposite. The contact forces will be treated as external forces acting on the body. As a result, the virtual work



a) Condition at contact



b) Forces acting on contactor and target bodies

Fig. 3.4 Schematic representation of contact conditions.

of these forces is incorporated in the formulation, as follow:

$$\Pi_1 = \Pi - \sum_{k} W_k \tag{3.1}$$

where:  $\Pi$  is the usual (incremental) total potential energy leading to the incremental equilibrium equations without contact conditions;

 $\sum_{k}$   $W_{k}$  is the incremental potential energy of contact forces; and k refers to a generic node k.

As Equation 3.1 shows, the virtual work of contact forces are added to the total potential energy of the system. Despite the simplicity of the concept, evaluation of  $W_k$  and determination of contact conditions along the contact surfaces are computationally very difficult.

To evaluate  $W_k$ , first, the contact forces must be determined. The contact forces are calculated based on the basic condition of contact along the contact surfaces, i.e., material overlap cannot occur. Based on this condition, during each equilibrium iteration, the most current geometry of the contactor and target surfaces is used to determine and eliminate the material overlap of the contactor nodes into the target nodes.

Understanding of the method of calculation of material overlap is beneficial in the modelling of the contact problem. Calculation of the material overlap at a generic two-dimensional contactor node k consists of the following steps:

- 1- Determining all possible target surfaces where node k can come into contact.
- 2- Finding the nearest local target node n to node k.
- 3- Determining if node k is in contact with the target body and evaluating the material overlap, using the local node coordinates k, n-1, n and n+1.

Determination of the contact conditions is another part of the formulation. Three types of contact conditions can be distinguished during each equilibrium iteration: 1) sticking; 2) sliding; and 3) separation of bodies (tension release).

Determination of the contact conditions needs the evaluation of surface tractions

and the application of certain criteria to them. The contactor surface tractions are calculated from the developed contactor surface nodal forces. The criteria are as follows:

- 1- If the total normal contact force over a segment of contactor surface is tensile, then tension release or separation occurs and both normal and tangential contact forces over the segment are then updated to zero for the next iteration. From this condition, it is evident that the normal contact forces can only be in the form of compression.
- 2- If  $|T_t| < \mu_s T_n$  (where  $T_t$  and  $T_n$  are tangential and normal surface tractions, respectively, and  $\mu_s$  is the static coefficient of friction), then there is no relative motion between two adjacent particles on the contactor and the target in contact which means that the sticking condition has occurred. Thus no updating of the segment normal and tangential tractions is performed by the algorithm.
- 3- If  $|T_t| > \mu_s T_n$ , then the segment experiences sliding contact. The tangential force is then updated to equal the segment frictional capacity (which is zero for the frictionless model and is equal to  $\mu_s T_n$  for the frictional model) and the direction of the force is set as the same as the direction after the previous iteration [28].

#### Comparison of the Two Methods

The main difference between these two formulations, based on their applications, is that in the case of contact modelling by using auxiliary elements, it must be known appriori which two nodes from the two bodies come into contact. This can raise some difficulties when there is some degree of uncertainty regarding the prediction of contact regions.

Another minor difference is that in the formulation without the auxiliary element, each one of the bodies considered in the analysis must be properly supported without including the contact conditions when static analysis is performed. In other words, the solution without contact must also be possible.

In this study, the finite element contact formulation implemented in the ADINA software based on the second method (which incorporates the concept of contact surfaces) was used for analysis. In addition to the advantage mentioned above, the frictional effects can easily be modelled by using this formulation.

#### 3.3 FINITE ELEMENT MODEL DESCRIPTION

#### **GEOMETRY DETERMINATION**

The methods of dimensional measurements range from simple to complex, conceptually and also experimentally. In general, the simpler methods are the more time-consuming ones. Basically, all of the methods of geometry measurements can be classified into two major groups:

a) destructive methods; and b) non-destructive methods

#### Destructive Methods

Use of these methods require destruction of the specimen. The common technique in this category is that of casting the specimen in a reference box. After removing the soft tissues and cleaning of the bone surfaces with methylalcohol and acetone, the clean bone is cast in a reference box with an appropriate material like polyester resin. The alignment of the bone inside of the box and establishment of a coordinate system, are the two important steps in this method. The cast specimen is then cut in serial sections of proper thickness and in the desired direction. Slide photographs can then be taken from these slices for digitization and measurement. Instead of photography, direct measurement or any other convenient method can be used at this stage.

#### Non-Destructive Methods

Non-destructive methods are normally preferred since the specimen is retained intact. However, most of these techniques demand sophisticated equipment.

The simplest method in this category uses a dial gauge, which is usually applied with a machine tool. Using a machine tool provides easy establishment of the coordinate

system. This method is, however, very time-consuming.

The more advanced methods involve optical techniques such as: moire photography, raster stereography, close-range photogrammetry and analytical stereophotogrammetry [33]. In the latter method, the 3-D image of an object is constructed based on the 2-D images taken by two cameras from two directions, by intensive mathematical computations.

Another method in this group considers the use of the CT-Scan, which is used mainly in medical applications such as brain tomography. Using this method, images of arbitrary transverse sections of an object can be obtained.

All these methods can be compared or classified based on the following criteria:

- a) accuracy;
- b) required equipment (cost and complexity);
- c) time consumption; and
- d) capability to asses the internal geometry.

The measurements obtained from all of the mentioned methods are accurate enough for use in the finite element analysis. But most of these techniques are only capable of surface profile measurements. There are one destructive (casting & cutting) and one non-destructive methods (CT-scan) which provide information also about the interior geometry and structure. By these methods the thickness of the cortical shell of the bone can also be estimated.

In this study, the dimensional measurements obtained in a previous study (in Biomechanics laboratory at McGill university) using CT-Scan method were used. Twelve X-ray CT-Scan images of transverse sections of the proximal portion of a tibial specimen of average size were obtained. The outlines of the cancellous and the cortical bones for each section were traced and digitized. The digitized points were then used to generate the finite element mesh.

#### MESH GENERATION

After determining the geometry of the proximal tibia as described in the above section, division of the volume of the tibia into discrete number of elements with proper size and shape is the next step in the finite element modelling process.

The process of constructing the finite element mesh using the geometry data can be performed in different ways ranging from manual to fully automatic mesh generation. In parallel to the intensive effort for the improvement of finite element algorithms to solve complex problems, the need for effective and time-saving methods of mesh generation has also prompted researchers to develop algorithms for automatic generation of two- and three-dimensional meshes. Up to date, these algorithms have been satisfactory mainly for two-dimensional geometries. Having a complex 3-D structure, the semi-automatic procedure incorporated in the FEMAP program (FEMAP is a pre- and post-processor for finite element analysis) was used to generate the mesh.

The prosthesis mesh was created by two short programs written in Fortran and FEMAP languages. These programs were suitable to generate mesh for any object which has bilateral symmetry. First, nodes and elements of one-quarter of the prosthesis were created. Then the nodal data of the rest were produced using FEMAP commands. The rest of the element data were generated by the Fortran program and were used as input to the FEMAP program to build the elements. A total of 398 nodes and 252 elements were generated for the prosthesis. Figure 3.5 presents the prosthesis geometry and mesh.

The mesh for the tibia was generated by building the transverse layers of elements, starting from the epiphysis and finishing at the distal end (93 mm down). Wherever possible, a layer of elements was copied to create the inferior layer. At some regions, this process required changes in size and shape of the elements. The top of the tibia was assumed to be flat with four holes at the corners corresponding to the design of the prosthesis.

A total of 1378 nodes and 1127 elements were created for the proximal tibia. The prosthesis and tibia together have 1776 nodes, 1379 elements, and 5244 degrees of freedom. The tibia mesh is shown in Figure 3.6.

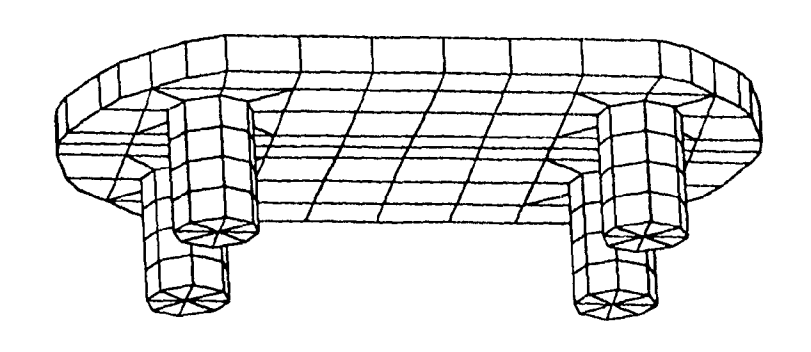


Fig. 3.5 The 3-D finite element mesh of the prosthesis.

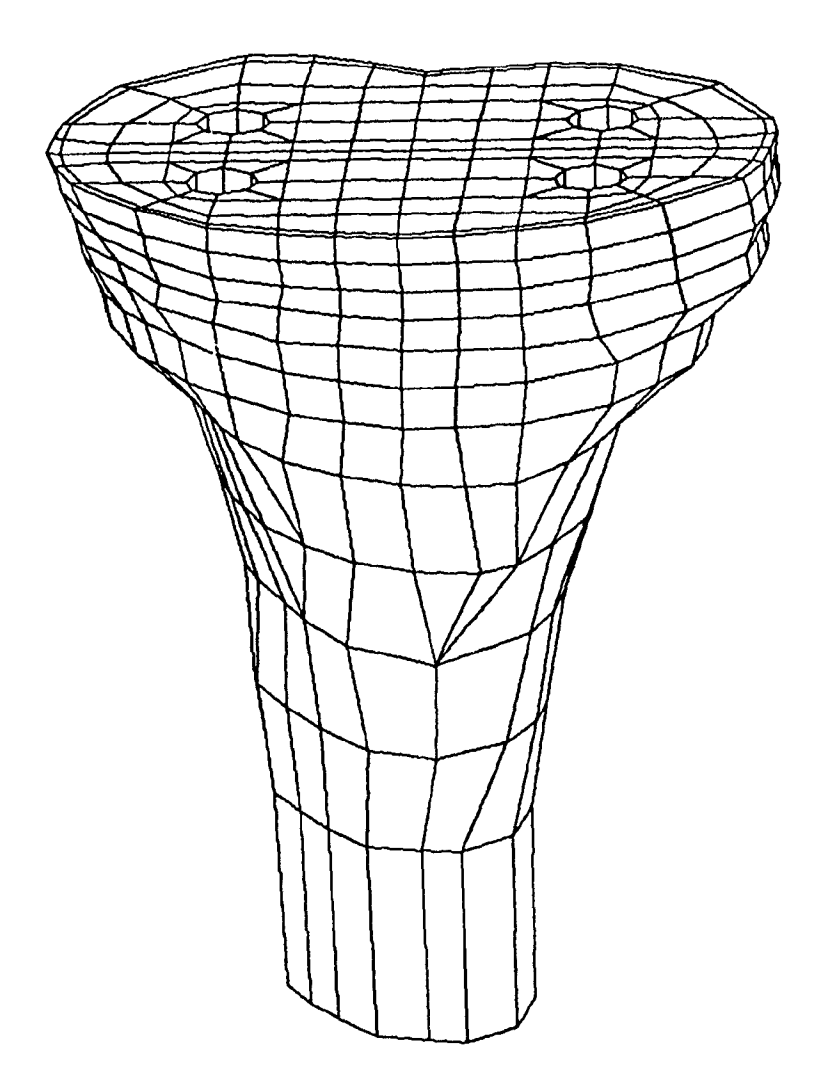


Fig. 3.6 The 3-D finite element mesh of the tibia.

### MATERIAL PROPERTIES

The response of the bone to an external load, like that of any structure, depends on the geometry or shape of the structure and the properties of the material from which it is made. Therefore, for the purpose of stress analysis, a knowledge of the material properties of bone is necessary.

The tibia consists of two types of bone, namely, cancellous and cortical bone. Cortical bone has a compact structure relative to cancellous bone. Cancellous bone has a porous structure formed by bone trabeculae. The modulus of elasticity of cortical bone can be approximately 10-300 times of that of cancellous bone. Cortical bone surrounds the cancellous bone like a hard shell.

In spite of the large difference in the material properties of the two types of bone, some researchers have recently attempted to consider cancellous bone as a porous structure comprised of bone tissues with the same microscopic mechanical properties as cortical bone [34]. In fact, the contrast between the material properties of cancellous and cortical bones is considered not due to the difference in tissue properties, but to the difference in density of the bone tissues. The relationship of the bone material properties to the density shows that all bone tissues are similar, whether it be in the form of cancellous or cortical bone. [22]

Many investigations have been done in order to correlate the modulus of elasticity and the strength of cancellous bone to its mineral density, porosity and orientation of the trabeculae. It has been established that porosity plays the major role [35].

Cancellous bone has a porous structure filled with a fatty viscous fluid. It has been shown that the mechanical properties of cancellous bone are similar to that of fluid-filled porous engineering material [29]. The preferred structural orientation of the trabeculae is the cause of the anisotropy in the material properties of cancellous bone.

In general, bone material has been known to be anisotropic, inhomogeneous, nonlinear and strain-rate dependent. Depending on the type of applied load (static or dynamic), direction and magnitude of the load and expected accuracy of results, simplifying assumptions of the material properties can be considered in the analysis. For instance, if the applied load is static, strain-rate dependency can be neglected. The assumption of isotropy, in cases when loading is in the direction of the longitudinal axis of the bone, has been shown to have little effect on the results [36]. In the same manner, bone can be considered to be a linear material if the level of the load is in the range of normal physiological loading where bone is known to actually respond in this manner [36].

It has been shown by previous finite element studies [36,43] that the effect of anisotropy of the cancellous bone on the results of finite element analysis is minor, provided that the inhomogeneity of the cancellous bone is taken into account.

Based on the above considerations, for this analysis, cancellous and cortical bones are assumed to be linear, isotropic, but inhomogeneous. Twenty-five different elastic moduli are assigned to the groups of elements belonging to the different regions of the tibia. Thirteen of these are allocated to the cancellous bone and 12 to the cortical bone.

A Poisson's ratio of 0.3 is chosen for both cancellous and cortical bones in the finite element model based on previous approaches for similar analyses by Little *et al*. [36] and Van Buskirk and Ashman [37].

### Elastic Moduli of Cancellous Bone

The elastic moduli of cancellous bone were taken from the literature [29]. The reported data for the elastic moduli were obtained from test results of five human tibiac (3 male, 2 female) between the ages of 50 and 70. Small cylindrical plugs of cancellous bone of the five specimens were removed from the transverse layers, 10 mm thick, at the proximal tibiae. Each plug was tested in uniaxial compressive stress at a strain rate of 0.1% sec<sup>-1</sup>.

To incorporate these elastic moduli into the finite element model, the plugs of each transverse layer were grouped according to the closeness of their elastic moduli. Then, an average elastic modulus was assigned for each group. The elements in each transverse layer of the tibia mesh were subsequently assigned the average elastic modulus of the corresponding group of plugs. These regions and the identification numbers

referring to the elastic moduli are shown in Figure 3.7 and Table 3.1.

### Elastic Moduli of Cortical Bone

Cortical bone forms the outer shell of the tibia. Geometrically, it is narrow at the epiphysis and becomes thicker at the diaphysis. In addition to dimensional variations, the material properties change as well. It has been found that the elastic modulus of cortical bone of long bones changes approximately linearly and increasingly from the epiphysis to the mid-diaphysis [31]. These results were found for bovine tibiae. In this study, it is assumed that the variation of the elastic modulus of the cortical bone of the human tibiae has the same trend, but the magnitudes of the elastic moduli were taken from other references [4,30]. The distribution of the elastic modulus of the cortical bone considered in the finite element model is shown in Figure 3.8 and Table 3.2.

### Material Properties of the Prosthesis

The prosthesis used in the experiment, was fabricated from steel and the material properties of steel (i.e. E=207000 MPa, v=0.3) was assigned to the prosthesis in the finite element model.

### **BOUNDARY CONDITIONS**

The contact formulation used in the ADINA program requires that each object in contact be restrained against rigid body motion. This is due to the fact that each object is analyzed separately by the program; however, the contact forces due to the interaction of objects are considered as external forces for each object. Therefore, the prosthesis was restrained by employing six auxiliary truss elements as shown in Figure 3.9. One end of each truss element was fixed and the other end was connected to the prosthesis. The stiffnesses of these elements were chosen to be very small, so that their effects on the prosthesis stiffness were negligible. However, for the tibia, the nodes at the distal end were restrained in all directions.

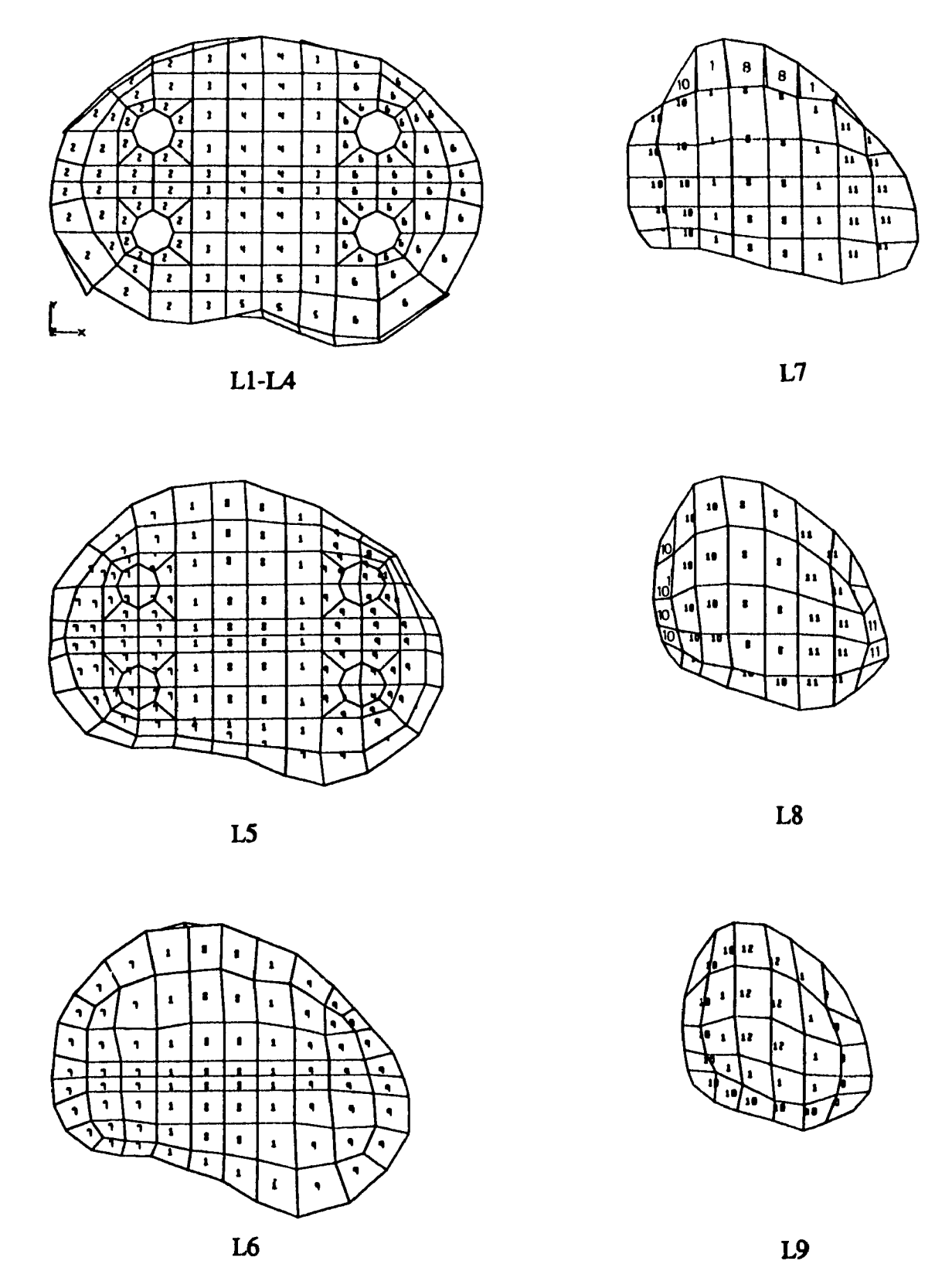


Fig. 3.7 Distribution of elastic moduli of cancellous bone.

(please refer to table 3.1 for the values of elastic moduli).

Material  Identification No.	E (MPa)
<u> </u>	100
2	210
3	160
4	60
5	100
66	300
7	165
8	40
9	195
10	130
11	180
12	25
13	80

 Table 3.1 The elastic moduli of cancellous bone.

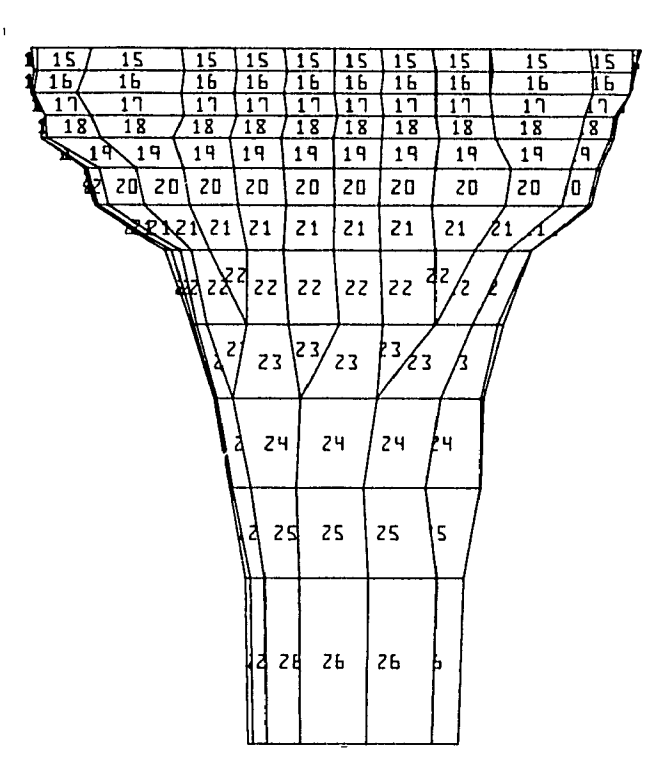


Fig. 3.8 Distribution of elastic moduli of cortical bone. (please refer to table 3.2 for the values of elastic moduli).

Material Identification No.	E (MPa)
15	1140
16	1420
17	1700
18	1980
19	2310
20	2730
21	3240
22	3990
23	4920
24	5950
25	7070
26	8650

Table 3.2 The elastic moduli of cortical bone.

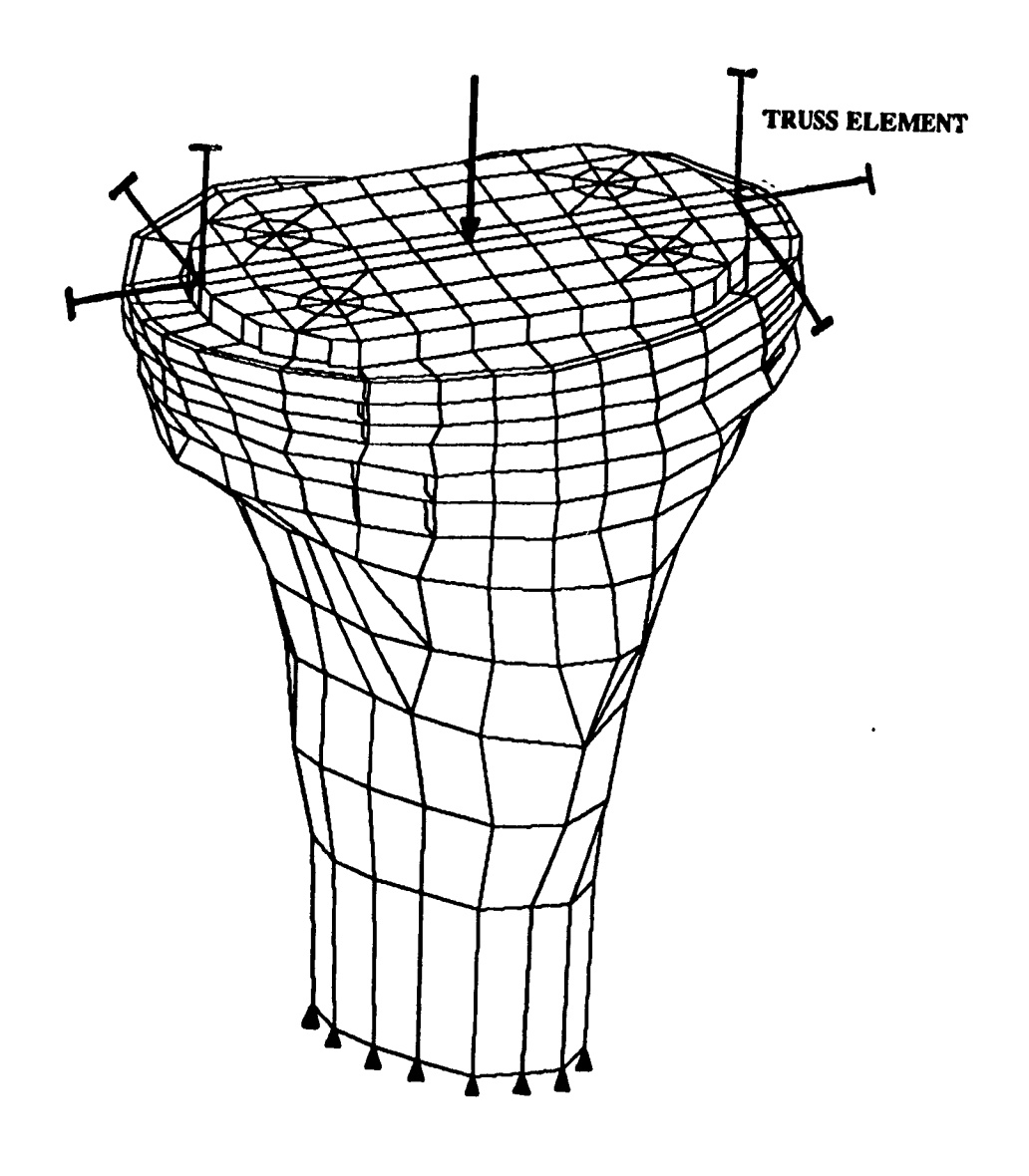


Fig. 3.9 Loading and boundary conditions.

### LOADING

As stated in Chapter 2, the forces transmitted across the knee joint range from two to seven times the body weight for normal activities. Since the evaluation of absolute values of the relative displacements was not the goal of this study, only a compressive load of 1000 N was applied at the central node of the prosthesis to compare the different fixation methods (Fig. 3.9).

### **ELEMENT TYPES**

The linear 8-node brick and 6-node wedge elements were used for constructing the model of the tibia and the prosthesis. The 6-node wedge elements were employed only at transition zones, where the cross sectional area changes. For all of the elements in the mesh, the aspect ratio and the distortion were less than 5 and 45 degrees, respectively. However, the elements with high aspect ratio and distortion were far from the regions of interest.

### CONTACT SURFACES

A total of 18 contact surfaces were defined for the prosthesis and the tibia, from which nine were specified as the contactor and nine as the target surfaces. It was found that different arrangements of the contact surfaces of the bone and the prosthesis as the contactor or the target surfaces, influence the convergence of the solution. For instance, in Figure 3.10, model (a) did not yield a converged solution, and model (b) converged faster than model (c). The option of different arrangements of the contact surfaces is useful for the modelling of certain conditions. For example, in modelling press-fit, the vertical surfaces of the bone holes were intentionally defined as contactor surfaces based on the treatment of the contactor nodes by the ADINA program. The reasons for this are explained in detail later in this Chapter.

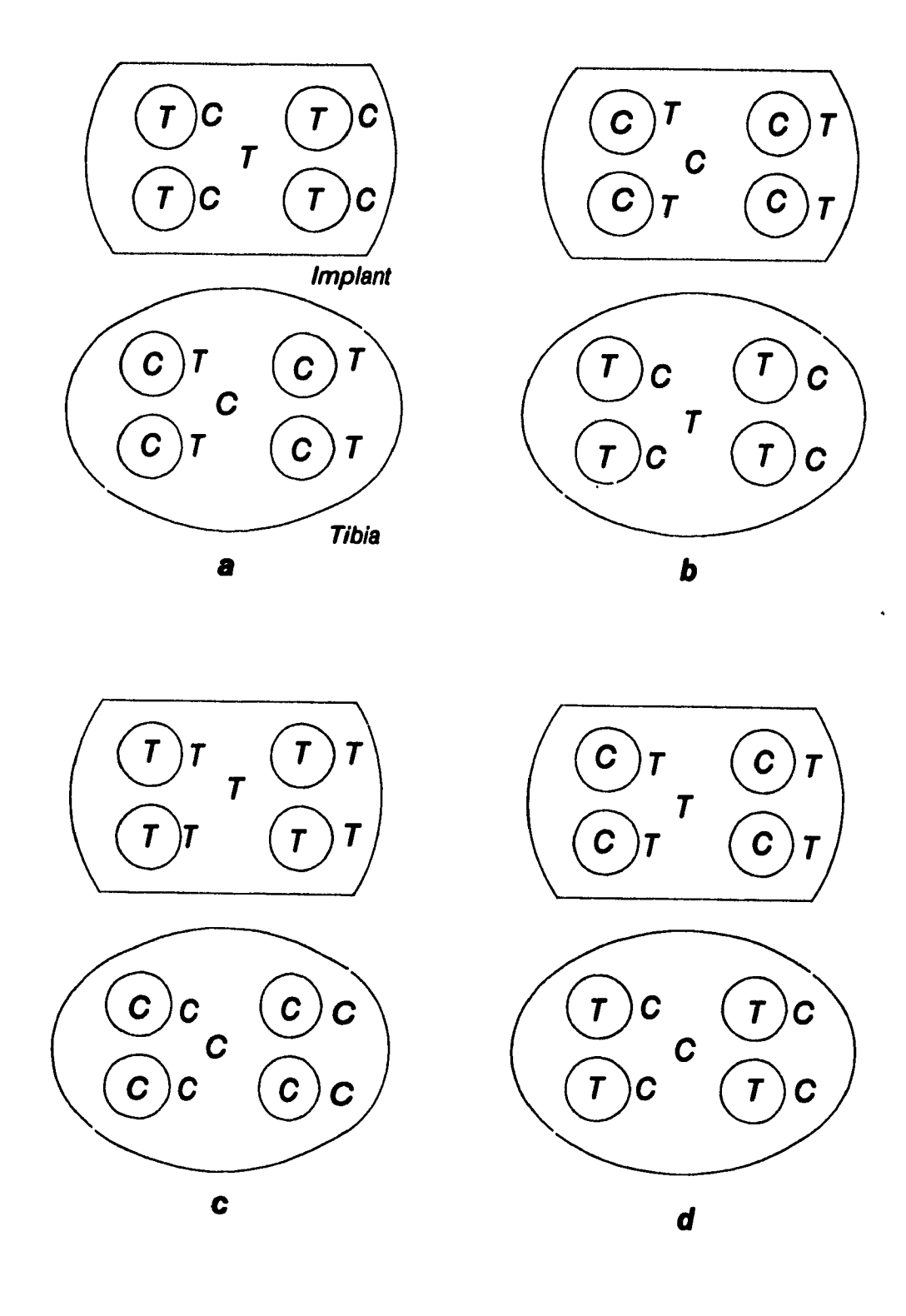


Fig. 3.10 Different arrangements of contactor and target surfaces.

### 3.4 PRESS-FIT AND SCREW FIXATION MODELLING

### PRESS-FIT MODELLING

When assembling two cylindrical parts by shrink-fit or press-fit, a contact pressure is created between the two parts. In obtaining a press-fit, the diameter of the male part is made larger than the diameter of the female part. The difference in these dimensions is called the interference, which is the elastic deformation that the two parts must experience.

The pressure or normal stress introduced at the interface can be obtained by the following equation [38]:

$$p = \frac{\delta}{\left[\frac{b}{E_b} \left(\frac{c^2 + b^2}{c^2 - b^2} + v\right) + \frac{b}{E_p} (1 - v)\right]}$$
(3.2)

where: p : pressure at interface

 $\delta$ : interference.

b : peg radius,

c: bone radius,

E<sub>b</sub>: modulus of elasticity of bone,

E<sub>p</sub>: modulus of elasticity of prosthesis,

 $\nu$ : Poisson's ratio.

In the case of press-fitting of the prosthesis into the bone, where the elastic modulus of the prosthesis is about 1000 times that of the bone, the second part of the equation can be neglected. In other words, it is assumed that the deformation of the peg is negligible with respect to that of the bone. Therefore, Equation 3.2 can be simplified as:

$$p = \frac{\delta}{\left[\frac{b}{E_b} \left(\frac{c^2 + b^2}{c^2 - b^2} + v\right)\right]}$$
(3.3)

Since the bulk of the bone surrounding each peg does not have a cylindrical shape, the methods of estimating a value for the radius of the surrounding bone is debatable. Figure 3.11 Shows the variation of pressure versus the bone radius. The curve (obtained using Equation 3.3 with the parameters: b=4 mm, and  $E_b=200$  MPa,  $\nu=0.3$ ,  $\delta=0.02$ mm) shows that the pressure reaches a constant value for a relatively small value of c. Hence,

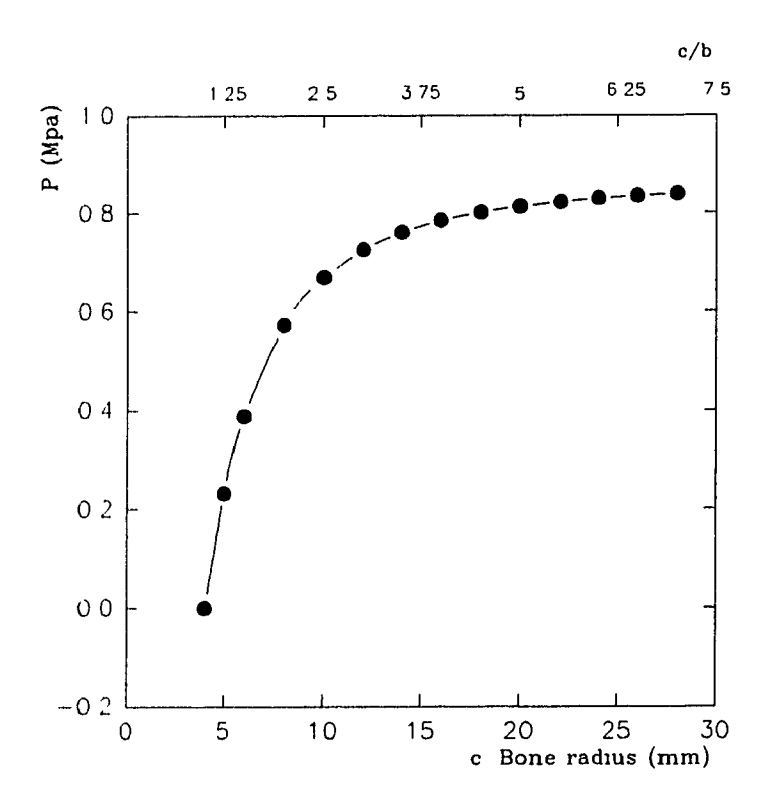


Fig. 3.11 The effect of bone radius on the pressure at the interface.

Equation 3.3 can be simplified assuming c approaches infinity. If  $\nu = 0.3$  then:

$$p = \frac{\delta E_b}{1.3b}; \tag{3.4}$$

Equation 3.4 is used for the verification of the finite element results of the press-fit model.

Finite Element Modelling of Press-Fit

The finite element formulation of the contact characteristic in the ADINA program does not allow overlapping of the contactor nodes into the target body. If the program detects such an overlap during any iteration, it eliminates the overlap and replaces it with the equivalent contact forces. The equivalent contact force is the force which produces elastic deformation equal to the overlap.

Based on this formulation, the press-fitting of the peg into the bone was modelled by overlapping the bone nodes into the peg. In this model, the contact surfaces of the bone's holes are considered as contactor surfaces. This implies that deformation occurs only at the bone side. An interference of 30  $\mu$ m was applied to the model of the press-fit. The overlap was half of the interference.

In the finite element model of the press-fit, some deformation is produced due to the elimination of the overlap of the bone nodes into the peg. Since in the physical model, the deformed state of the body due to press-fitting is the reference for the measurement of relative displacement, in the finite element model the initial displacements should not be taken into account for the evaluation of relative displacements. Therefore, the initial displacements were found and then were deducted from the corresponding displacements obtained in reference to the external load (i.e. 1000 N). This was done by application of the load in two steps, one for 100 N and another one for 1000 N. According to the results of the two analyses and assuming a linear relationship for load and displacement, the displacement in the absence of any external load, i.e., the displacements due only to the elimination of overlapping, were

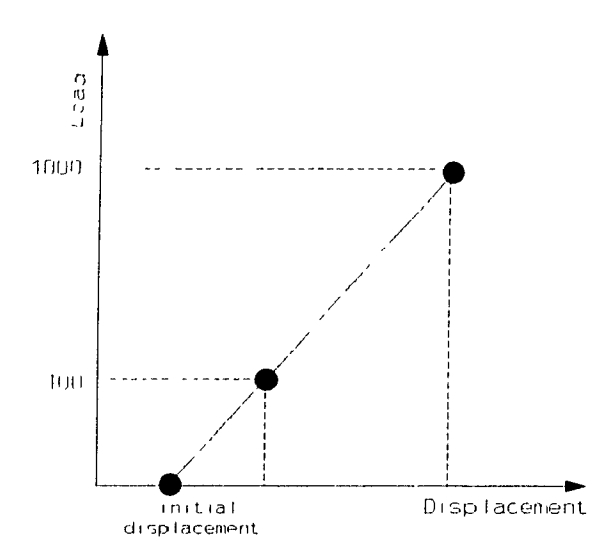


Fig. 3.12 Initial displacement due to press-fit.

### SCREW FIXATION MODELLING

Screw fixation was modelled based on the effect of the screw in producing an initial compressive force at the horizontal interface of the bone and prosthesis. Because of friction, this compressive force introduces a frictional force (tangential force) at the interface, which in turn reduces the relative displacement between the bone and prosthesis. By increasing the coefficient of friction of the horizontal interface in the finite element model, the effect of the compressive force can be modelled. Since the external compressive load also causes a tangential force at the interface, an equivalent coefficient of friction can be defined. The equivalent coefficient of friction represents the frictional effect of the compressive force caused by the screws and the external compressive load. The calculation of the equivalent coefficient of friction at the horizontal interface of the bone and prosthesis is shown below.

If,  $F_s$ : total compressive force produced by screws,

F<sub>a</sub>: total applied force (compressive),

F<sub>t</sub>: frictional force due to compressive force of the screws,

 $\mu$ : coefficient of friction between the bone and prosthesis, and

 $\mu_{\rm e}$ : modified or equivalent coefficient of friction,

then:

$$F_t = \mu F_s; \tag{3.5}$$

$$\mu F_a + \mu F_s = \mu_e F_a \tag{3.6}$$

$$\mu_e = \mu (1 + \frac{F_s}{F_a}) \tag{3.7}$$

The equivalent coefficient of friction obtained by Equation 3.7 is assigned for the tibial plateau in the finite element model.

To determine the compressive force caused by the tightened screw, the following equation can be used [38]:

$$F = \frac{T}{Kd} \tag{3.8}$$

K is a constant which depends on the screw specifications and is given by:

$$K = \left(\frac{d_m}{2d}\right)\left(\frac{\tan\lambda + \mu \sec\alpha}{1 - \mu \tan\lambda \sec\alpha}\right) + 0.625\,\mu_c \tag{3.9}$$

where: T: torque

d<sub>m</sub>: mean diameter of screw (4.8 mm)

d: major diameter (6.5 mm)

 $\lambda$ : lead angle (7°)

 $\alpha$ : thread angle (30 °)

 $\mu$ : coefficient of friction between bone and screw (0.15) taken from literature [39]

 $\mu_c$ : coefficient of friction between screw and prosthesis (0.6) (the screw specifications given above are measured from the screw used in the experiment)

To evaluate the magnitude of the torque (T), a preliminary test was performed on one specimen. The screws were tightened by two fingers (thumb and pointer) and a screw driver, a common method practised by surgeons, until either the screw was overtightened or the maximum power of the two fingers was applied by the experimentalist. The torque was obtained from averaging the torques measured for tightening the screws of the prosthesis. The results of several tests on different locations at the tibial plateau yielded an average torque of 0.576 N.m (5 lb.in). This magnitude of torque was used in the above equation and also was used for tightening the screws of the screw fixation in the experiment.

The physical body of the screw in the bone was modelled by a cylinder with a diameter equal to the mean diameter of the screws. The cylinders were considered to be fixed (no interface) to the prosthesis plate. Therefore no relative displacement was considered between the screws and the plate. The interaction between the screw teeth and the bone which restrains the relative displacement of the screw and the bone in the z-direction (direction parallel to the longitudinal axis of the screw) is not modelled in this study. This effect, which prevents separation of the bone and the prosthesis at the horizontal interface, becomes important under eccentric loading when separation is likely to occur. Due to the type of loading used in this analysis (i.e. central load), it is believed that the omission of this screw effect has little influence on the results.

# CHAPTER 4

## FINITE ELEMENT RESULTS

### 4.1 INTRODUCTION

In this chapter, the reliability of the finite element model is first evaluated by verifying the local and overall equilibrium and, wherever possible, by comparing the results with those of previous studies. The predictions of the proposed finite element models for the three types of fixation are then presented and some of them are compared to available analytical solutions. The three fixation methods analyzed here are: intimate or close-fit, press-fit and screw fixations.

Displacement, relative displacement and contact forces at the bone-prosthesis interface are typical results which are reported in this chapter. It must be noted that due to the large volume of results, it is not only impractical to present all results, but also it is unnecessary in some cases.

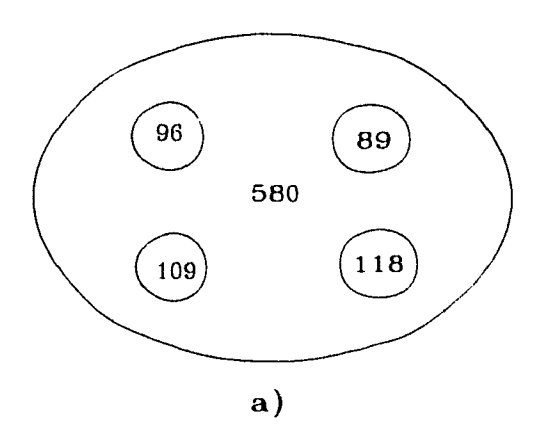
### **4.2 VERIFICATION OF RESULTS**

The first step in the verification of the finite element results is to check the overall equilibrium. The output of the finite element model shows that the summation of the reaction forces at the fixed nodes of the distal tibia is 998 N which is reasonably close to the applied external force (1000 N). It has to be noted also that the reaction forces in the six truss elements which connect the prosthesis to the two fixed points were

negligible (maximum 0.09 N) as expected. Truss elements were used in the model to restrain the prosthesis against rigid body motion. This was necessitated by the fact that the particular finite element formulation of contact requires that each body in contact be fixed against rigid body motion. In fact, the finite element routine analyzes each body separately but considers the effect of bodies on each other in the form of contact forces as previously described in Chapter 3. The truss elements were chosen to have a very low stiffness so that their effect on the stiffness of the prosthesis is negligible.

In models which include contact surfaces, a further verification would be to evaluate the local equilibrium. The local equilibrium is the balance of forces on each body in contact. These forces comprise of external, reaction and contact forces. Figure 4.1 shows distribution of the contact forces on the surfaces of the prosthesis which are in contact with the bone. Since the presented results belong to the analysis which did not include any frictional effect, no tangential forces exist on the contact surfaces. Summation of the contact forces in the z-direction shown in Figure 4.1a is 992 N which is close to the applied external force (0.8% difference). Also the summation of the contact forces in the y-direction shown in Figure 4.1b is close to zero (3.4% difference). This is reasonable because there are no external forces in the y-direction. From these results it is concluded that both local and overall equilibrium are satisfied.

Next, the results obtained in this study are compared against a number of existing finite element analyses. However, due to differences in geometry, material properties, prosthesis configuration and methods of analysis, some differences in the comparison are to be expected. The closest study to the current research is the one performed by Tissakht *et al.* [5] which used the same geometry, but a two-pegged prosthesis, different material properties and a different method of analysis using gap elements at the interface. Tissakht *et al.* obtained relative displacements at the outer edge of the prosthesis of up to  $27 \mu m$  under a central load of 1000 N; however, in the present model which uses a four-pegged prosthesis and considers interface friction, a maximum relative displacement at the same region was found to be only 8  $\mu m$ . Apart from differences in material properties, the stronger fixation obtained by the additional two pegs is believed to be the



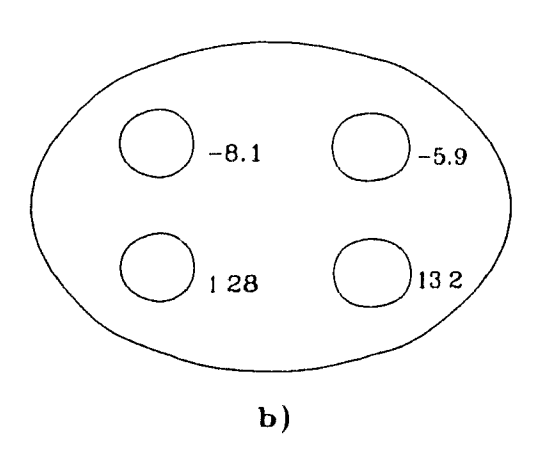


Fig. 4.1 Contact forces at interfaces (N).

- a) Contact forces at the horizontal interface in z-direction.
- b) Contact forces at the vertical peg-hole interface in y-direction.

main cause of this large difference between the above results.

### 4.3 INTERPRETATION OF RESULTS

Non-linearity of the load-displacement relation was checked by solving for three load steps (660,1000,2000). Figure 4.2 shows the displacements and the relative displacements for two typical points at the anterior and posterior edges of the prosthesis-bone horizontal interface. It can be seen that the degree of non-linearity differs for different locations but is generally small. Non-linearity in load-displacement relation is due to the existence of contact conditions in the model. Due to closure of a gap or separation of contact surfaces the stiffness changes, which, in turn, results in a non-linear relation of load and displacement.

For the first time in the finite element analysis of the prosthetically resurfaced tibia, frictional effect at the interface is taken into account. There are not much data available regarding the coefficient of friction between the prosthesis and bone. The only work in this field has been reported by Shirazi-Adl et al. [39,40]. The authors determined the frictional properties at the interface between bone and prosthesis material of porous and smooth surfaces. Shirazi-Adl et al. found that friction curves (representing the variation of friction with relative displacement) are highly non-linear and do not conform to Coulomb's law of friction where displacement does not occur before the maximum resistance force is reached. For the smooth surface, according to Shirazi-Adl et al., the coefficient of friction ranges from zero to 0.42 depending on the range of the relative displacement. According to the range of the relative displacement predicted by the finite element analysis of the resurfaced tibial model without friction, a coefficient of 0.15 was selected from the friction curve for a smooth surface presented in their report [39]. However, the finite element analysis was done for a number of values of the coefficient of friction in order to determine the effect of friction on the relative displacement at the interface of the bone and the prosthesis. Figure 4.3 shows the interface relative displacement as a function of the coefficient of friction for 4 different points at the interface (whose locations are shown in the same figure) with very different

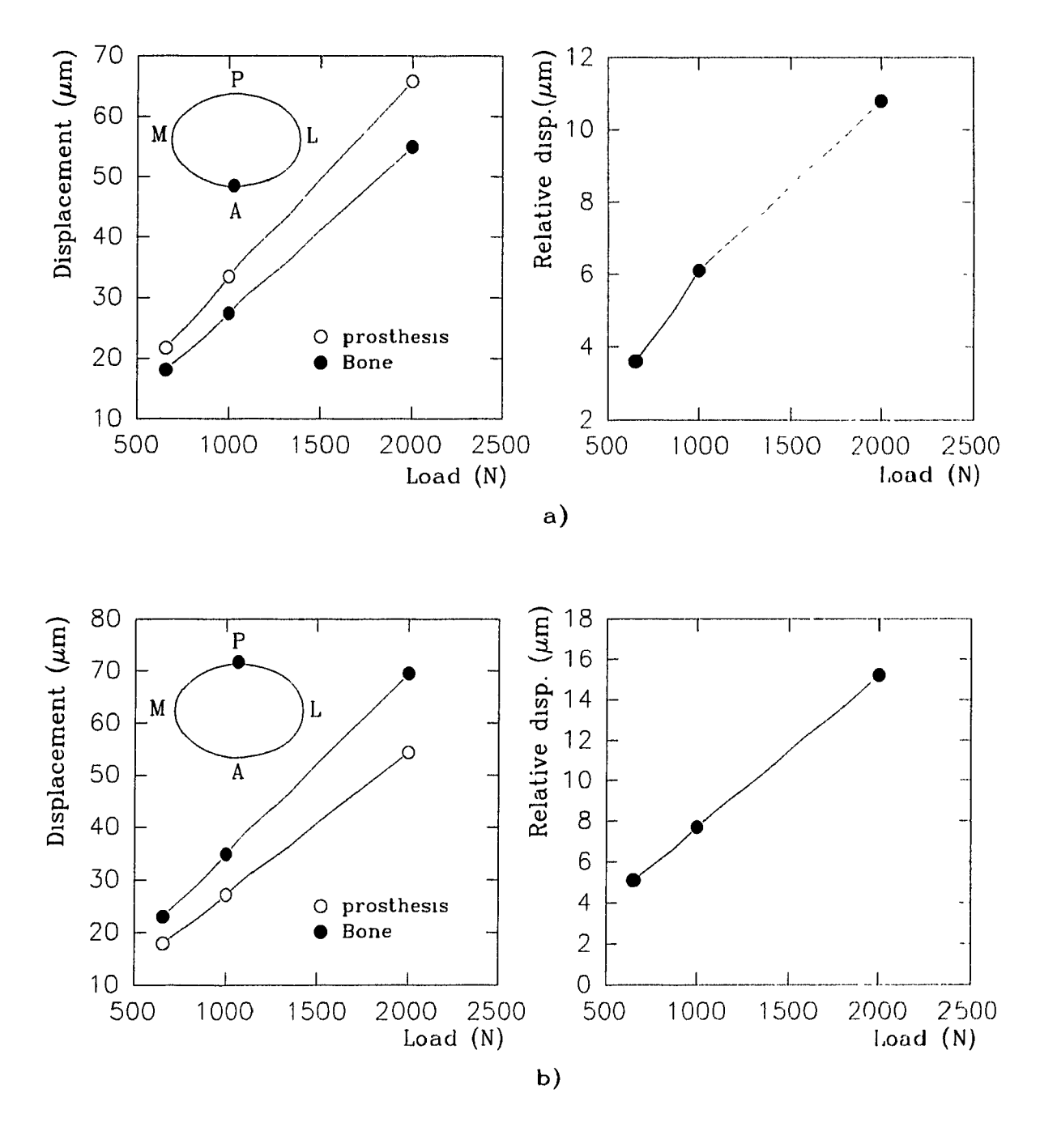


Fig. 4.2 Load-displacement relation for the bone-prosthesis interface.

a) a point at anterior side

b) a point at posterior side

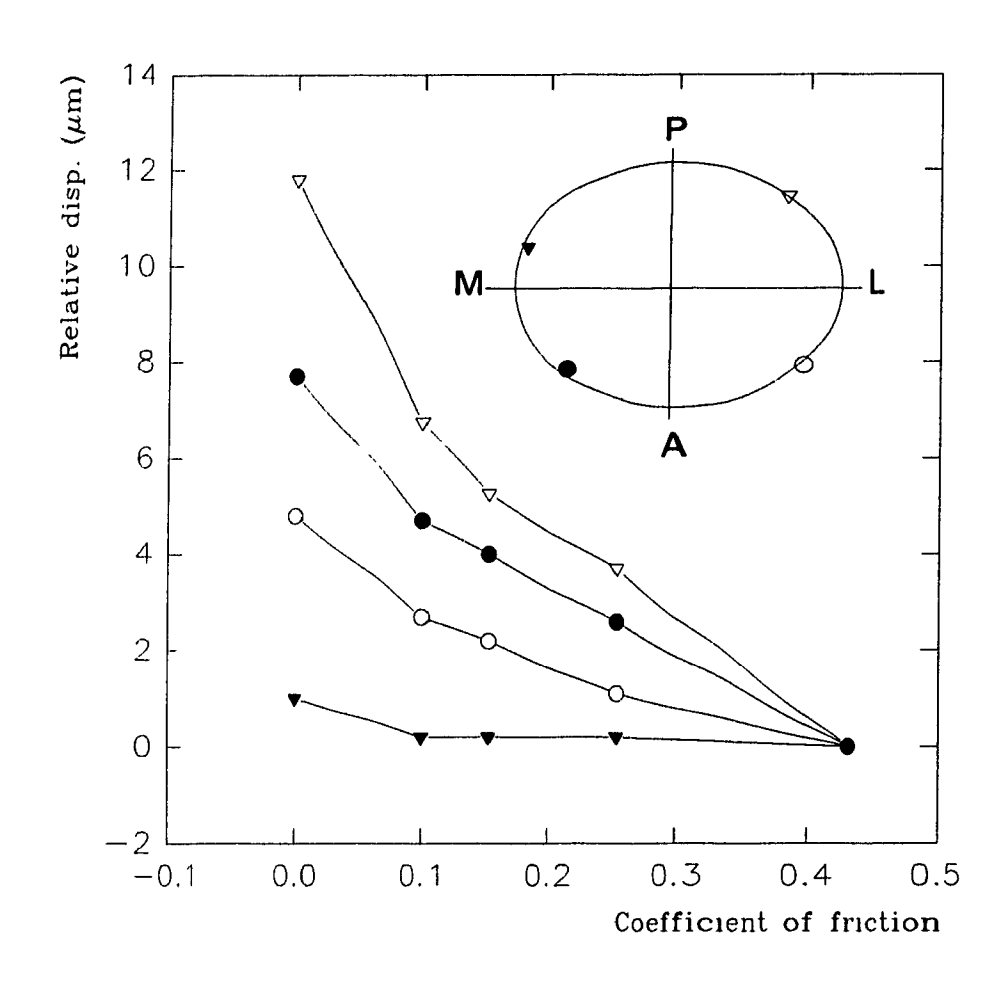


Fig. 4.3 Effect of friction on the relative displacement at the bone-prosthesis interface (load: 1000 N).

values of the relative displacement. The figure indicates that the relative displacements for all four selected points approach zero for a coefficient of friction of about 0.4.

### COMPARISON OF THE FIXATION METHODS

Having established the general validity of the finite element model developed in this study, three types of fixation were analyzed which are: intimate-fit or close-fit, press-fit, and screw fixation. In fact, the first model, i.e., the model with close-fit fixation, represents a reference condition with which the other two types are compared. In the close-fit fixation model, the initial distance between the corresponding target and contactor nodes is zero. The basics for the finite element modelling of these fixations were covered in the previous Chapter.

For all fixation models, the relative displacement at the horizontal interface was found to have high magnitudes at the anterior and posterior edges of the prosthesis which then decreases towards the centre of the prosthesis and around the pegs. For the close-fit and press-fit fixation models, the relative displacement at the edges of the prosthesis was also higher than those at the vertical peg-hole interface.

The majority of the results presented here correspond to the nodes at the anterior edge of the prosthesis-bone interface, a location where measurements were also performed. However, whenever deemed important, the results corresponding to other nodes are also presented.

### Close-fit Fixation Model

Figure 4.4 illustrates the finite element predictions of the displacements and the relative displacements for the close-fit fixation model, under a central load of 1000 N, without friction. The left column shows the displacements of the bone and prosthesis nodes along the interface in the x-, y-, and z-directions and the right column shows the relative displacements (which are the differences between the two plots of the left column). The displacements of the prosthesis and bone in the x-direction are in the range

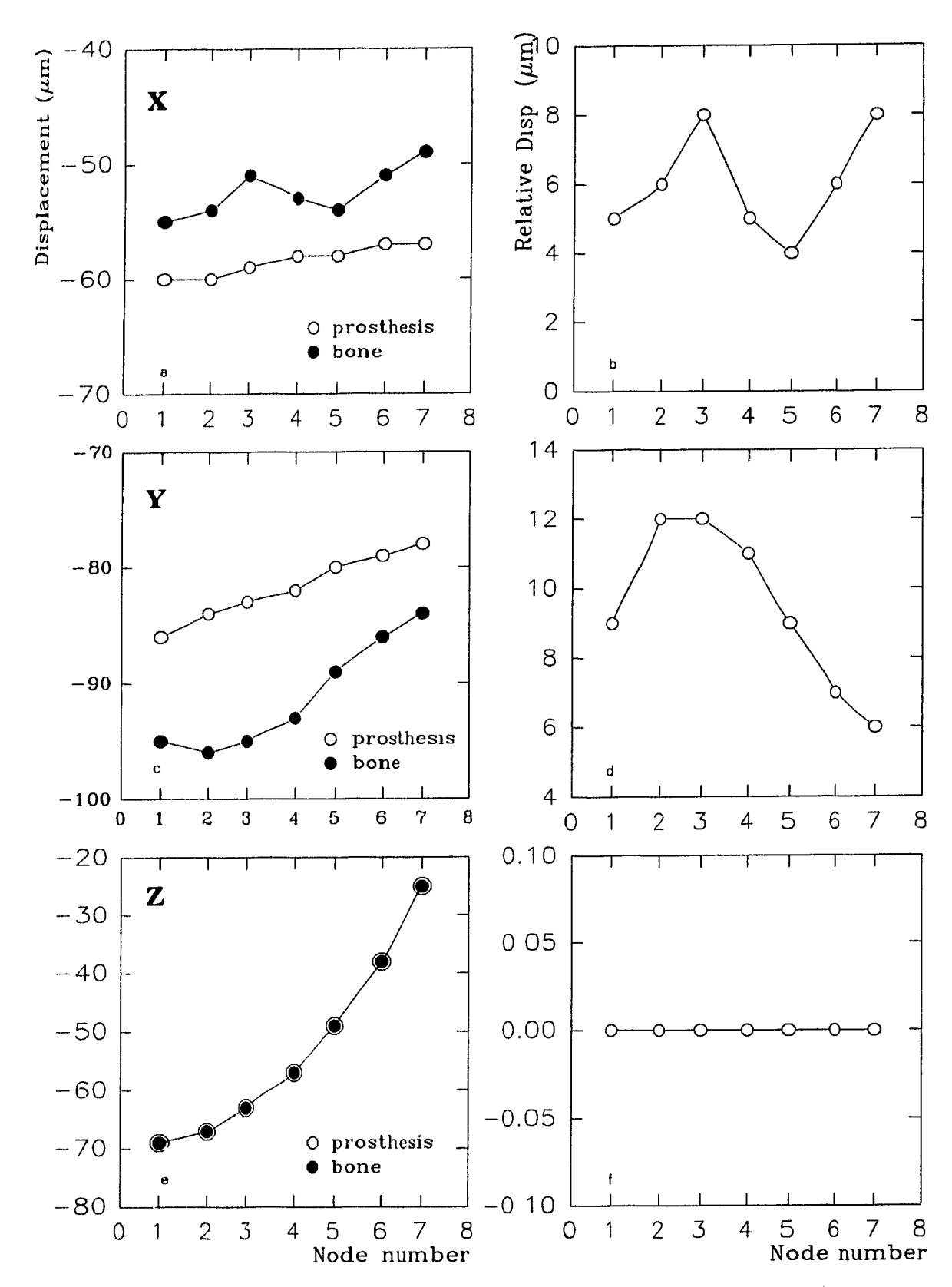


Fig. 4.4 Displacements and relative displacements at the horizontal interface for the close-fit model without friction.

50 to 60  $\mu$ m (Fig. 4.4a). The displacements of the prosthesis in the x-direction differ only slightly for the seven nodes, which implies that the prosthesis experiences very small deformation. The maximum relative displacement in the x-direction is 8  $\mu$ m (Fig. 4.4b). Both, the displacements and relative displacements in the y-direction (Fig. 4.4c and d), are larger than those in the x-direction (by about 50%).

The displacements in the z-direction (Fig. 4.4e) are equal for both prosthesis and bone. This implies that the nodes of the prosthesis neither separate from nor penetrate into those of the bone. The displacements in the z-direction along the interface are not equal. This means that the tibia is deflected due to a bending moment (a difference of 50  $\mu$ m is seen between the displacements of the medial and lateral sides). This, in turn, implies that, in the model, the direction of the central load did not conform exactly with the neutral axis of the tibia.

In Figure 4.5 the finite element predictions for the frictional model of the close-fit fixation are shown in a similar manner to those for the frictionless model (Fig. 4.4). It is seen that the pattern of the plots of the relative displacements in the x- and y-directions in the two figures are similar but the magnitudes of displacements for the tibia are closer to those of the prosthesis in the results of Figure 4.5. The displacements in the  $\lambda$ -direction are the same for both models (Figs. 4.4e and 4.5e).

## Comparison of the Close-fit and Press-fit Fixation Models

In Figure 4.6 the finite element predictions for the press-fit fixation model are shown in the same manner as in Figures 4.4 and 4.5. The interface friction was taken into account for the analysis of the press-fit fixation model. In comparison to the close-fit model, a decrease in the relative displacement in the x-direction and an increase in the y-direction is seen (this comparison is shown in Fig. 4.7). The displacements in the z-direction are the same for the close-fit and the press-fit fixation models.

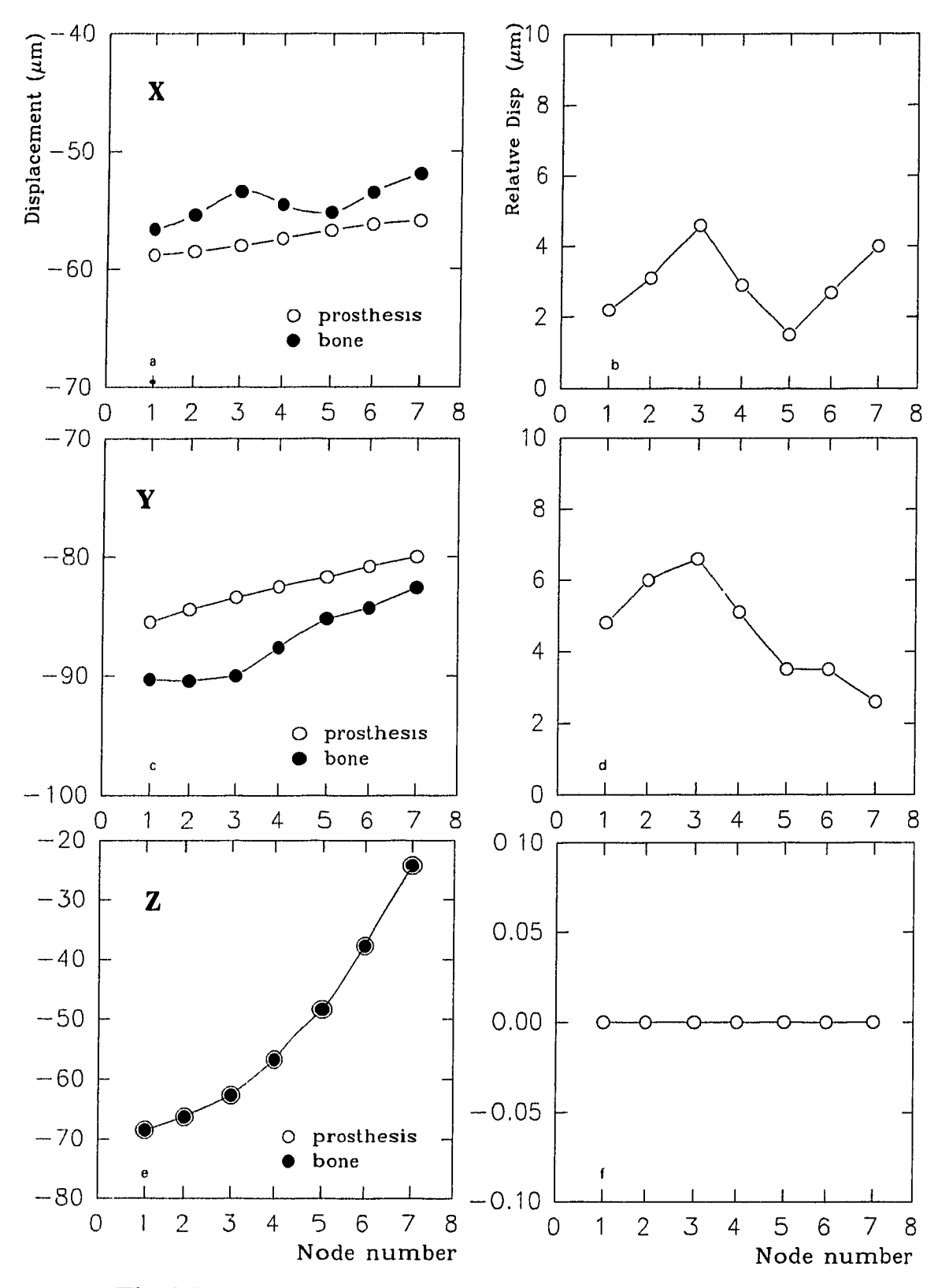


Fig. 4.5 Displacements and Relative displacements at the horizontal interface for the close-fit model with friction.

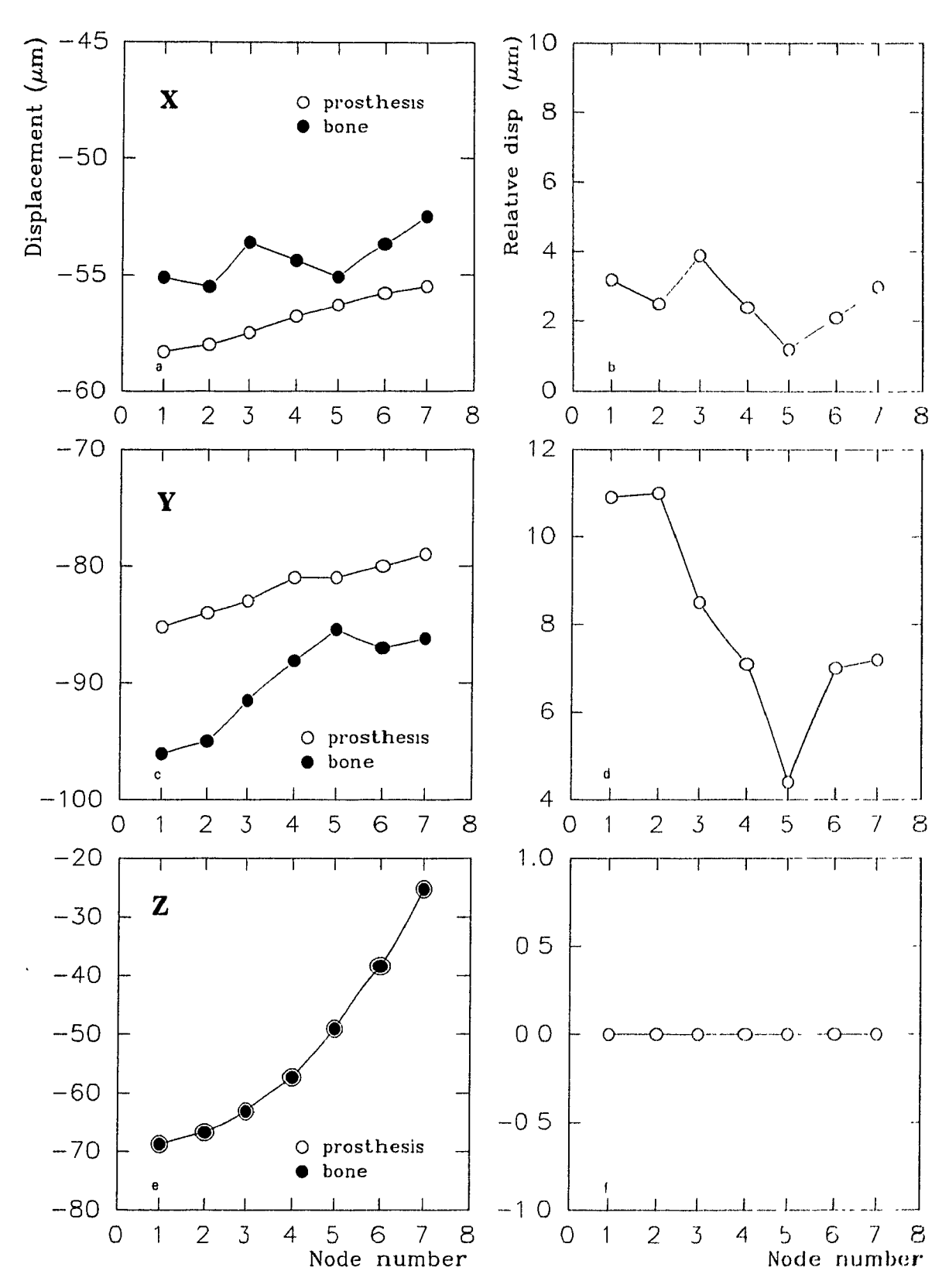


Fig. 4.6 Displacements and Relative displacements at the horizontal interface for the press-fit model.

The relative displacements at the horizontal interface for the close-fit and press-fit fixations, in the x- and y-directions, are compared in Figures 4.7a and 4.7b respectively.

Figure 4.7a shows that except for one node, the pattern of relative displacements for the press-fit and close-fit models are similar. On average, the relative displacements in this direction are about 20% smaller than those for the close-fit fixation model. The pattern of relative displacements for the two fixation models in the y-direction (Fig. 4.7b) are less similar than those in the x-direction. In addition, the relative displacements in the y-direction for the press-fit fixation model are larger than those for the close-fit model (by about 70%). The total relative displacements (summation of relative displacements components in the x- and y-directions) for the press-fit fixation model are larger than those for the close-fit fixation model.

In Figure 4.8 the relative displacements at the peg-hole vertical interface for both the close-fit and press-fit fixation models are compared. The relative displacements for the press-fit fixation model are about 40% smaller than those for the close-fit fixation model. Smaller relative displacements predicted for the press-fit model is in agreement with larger contact pressures at the peg-hole interface for the press-fit model. Increase in contact pressures for the press-fit model causes an increase in the frictional forces which, in turn, decreases the relative displacements. Larger contact pressures at the peg-hole interface for the press-fit model is due to the elimination of the material overlap (interference) at this interface.

In Figure 4.9a and 4.9b the magnitudes of the normal contact forces at the horizontal interface and at the bottom of the pegs for the close-fit and press-fit models are shown respectively. As can be seen, the normal contact forces at the horizontal interface for the press-fit model are about 11% smaller than those for the close-fit model. This is in agreement with the larger relative displacements at this interface for the press-fit model. Reduction of the normal contact forces for the press-fit model results in a

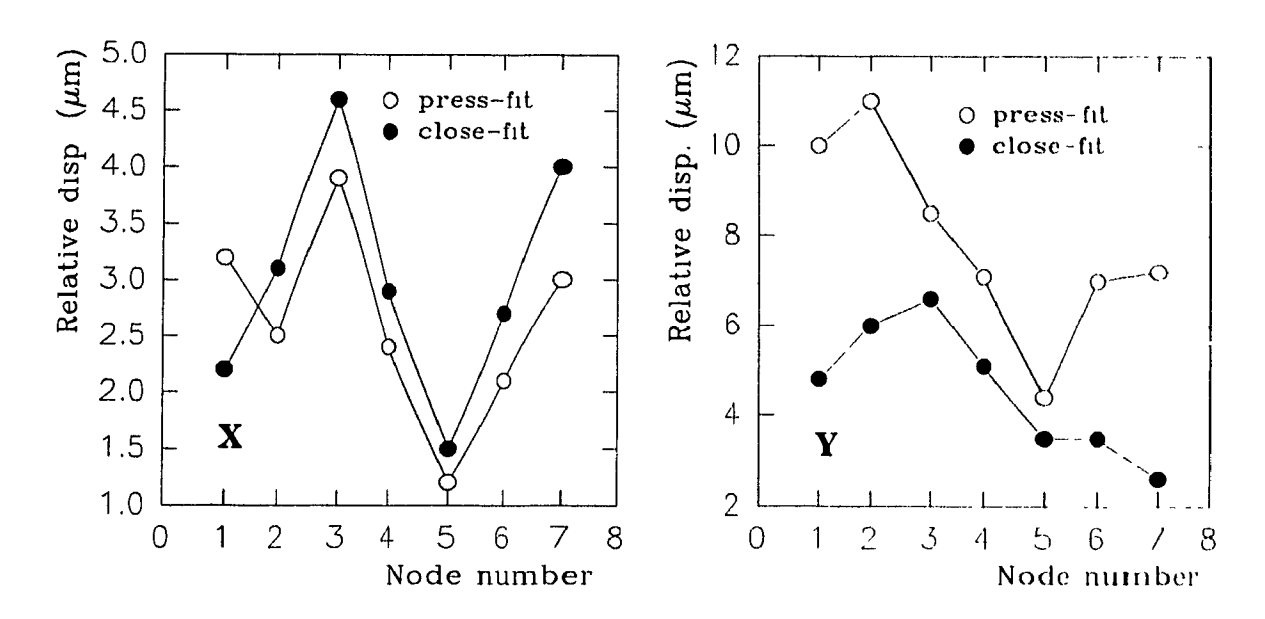


Fig. 4.7 Comparison of relative displacements at the horizontal interface for the close-fit and the press-fit models.

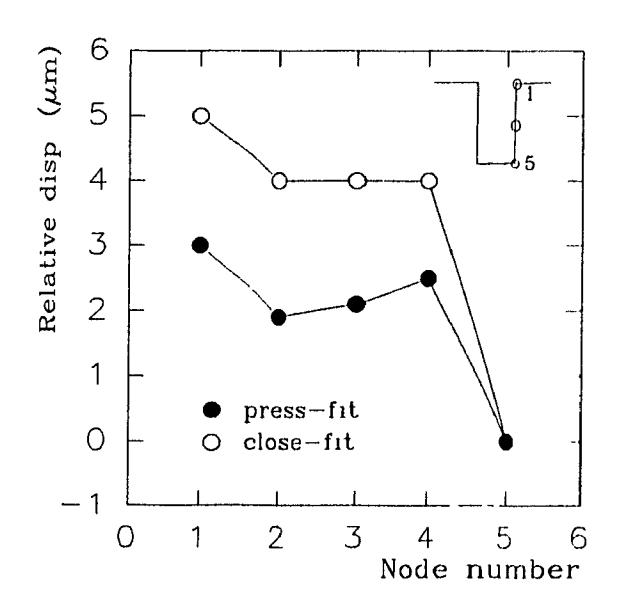
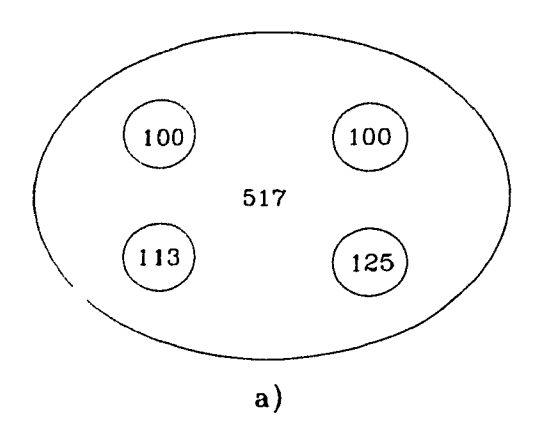


Fig 4.8 Comparison of relative displacements at the vertical peg-hole interface for the close-fit and the press-fit models.



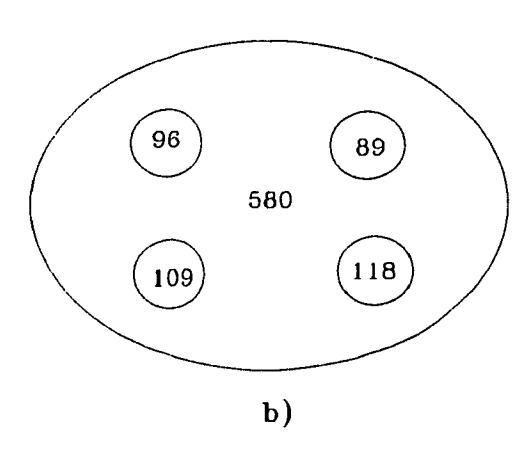


Fig. 4.9 Comparison of contact forces at the horizontal interface for the close-fit and the press-fit models (N).

- a) Press-fit model.
- b) Close-fit model.

decrease of the tangential (frictional) forces at the horizontal interface which, in turn, causes an increase in the relative displacements at this interface.

In Figure 4.10 the finite element predictions of contact pressures at the peg-hole vertical interfaces for the press-fit model are compared with those obtained using Equation 3.4 (the analytical solution to press-fitting of two cylinders). It is seen that the predictions of the finite element analysis of contact pressures are about 25% larger than those obtained by Equation 3.4. It has to be noted that the finite element predictions shown in the figure are the averages of the contact pressures on the segments around each peg. Also, as explained in Chapter 3, Equation 3.4 is an approximate form of the exact solution (i.e. of Equation 3.2).

The contact pressures at the medial side are higher than those at the lateral side.

This is due to the higher modulus of elasticity of the bone in the medial side relative to that in the lateral side of the tibia.

### Comparison of the Close-fit and Screw Fixation Models

In Figure 4.11 the finite element predictions of the displacements and the relative displacements at the horizontal interface for the screw fixation model are shown. The displacements of the prosthesis nodes in the x- and y-directions (Fig. 4.11a and c) are close to those for the close-fit and press-fit fixation models. However, the displacements of the bone nodes are predicted to approach the displacements of the prosthesis nodes, and at three nodes they are exactly the same. The relative displacements in the x- and y-directions (Fig. 4.11b and d) are significantly smaller than those for the close-fit and press-fit fixation models. The comparison of these relative displacements for the screw and close-fit fixation models is shown in Figure 4.12. The displacements in the z-direction (Fig. 4.11e) remain unchanged in comparison with those for the close-fit and press-fit fixation models.

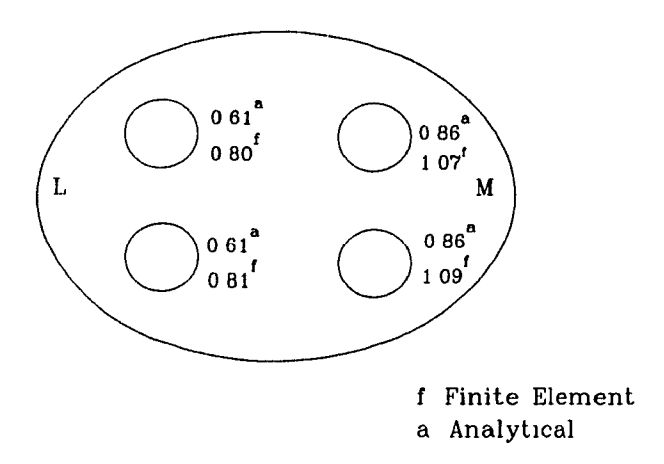


Fig 4.10 Contact pressures at the peg-hole interface due to press-fit (MPa).

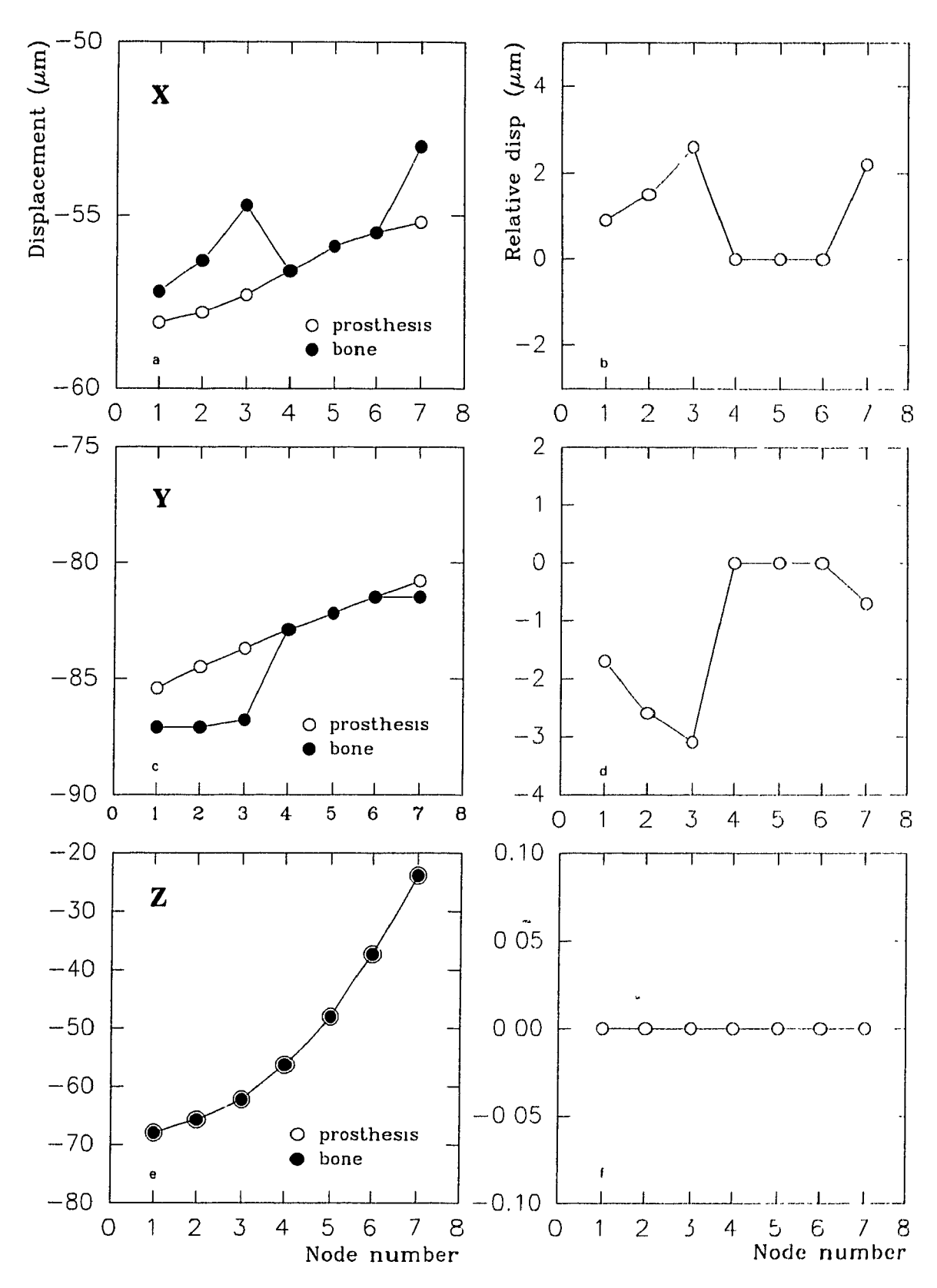
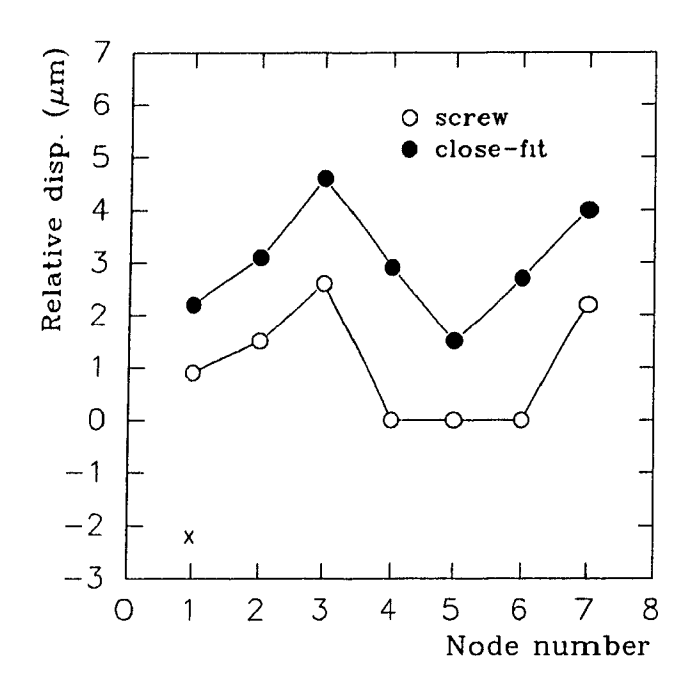


Fig. 4.11 Displacements and relative displacements at the horizontal interface for the screw fixation model.



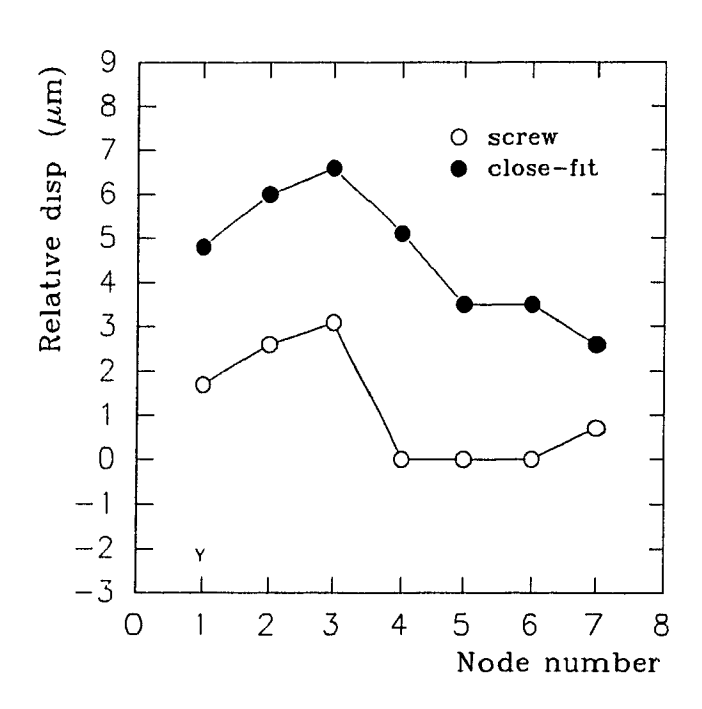


Fig. 4.12 Comparison of relative displacements at the horizontal interface for the close-fit and the screw fixation models.

The finite element predictions of the relative displacements at the horizontal interface for the close-fit and the screw fixation models are compared in Figure 4.12. The relative displacements in the x- and y-directions for the screw fixation model are less than half of that for the close-fit fixation model. The smaller relative displacements predicted by the screw fixation model is not surprising, because of the manner in which it was modelled. The modelling was based on the fact that a tightened screw introduces an initial compressive force at the interface which, in turn, causes a tangential (frictional) force against relative displacement between the bone and the prosthesis.

## THE EFFECT OF THE LENGTH OF THE TIBIA ON THE RELATIVE DISPLACEMENT

Figure 4.13 shows the finite element predictions of displacements, in the x- and y-directions, of the nodes along the tibial axis for the close-fit fixation model. The curves with filled circles represent polynomial functions in which the displacement is proportional to the square of the distance from the fixed end of the tibia. It is seen that these curves can closely be fitted to the curves representing the finite element results. It is interesting to note that the deflections along the longitudinal axis of a cantilever beam is also proportional to the square of the distance from the fixed end of the beam.

Although load is applied at the centre of the prosthesis, this variation of the displacements along the tibial axis in the x- and y-directions indicates that the centre of the prosthesis does not conform to the tibial axis and hence, the load introduces a bending moment.

Based on these results it can be asserted that the displacements and relative displacements at the interface are highly dependent on the length of the tibia considered in the model. The length of the tibia is a parameter which was neglected or was given inadequate attention in previous studies. In fact, the proximal tibial model underestimates

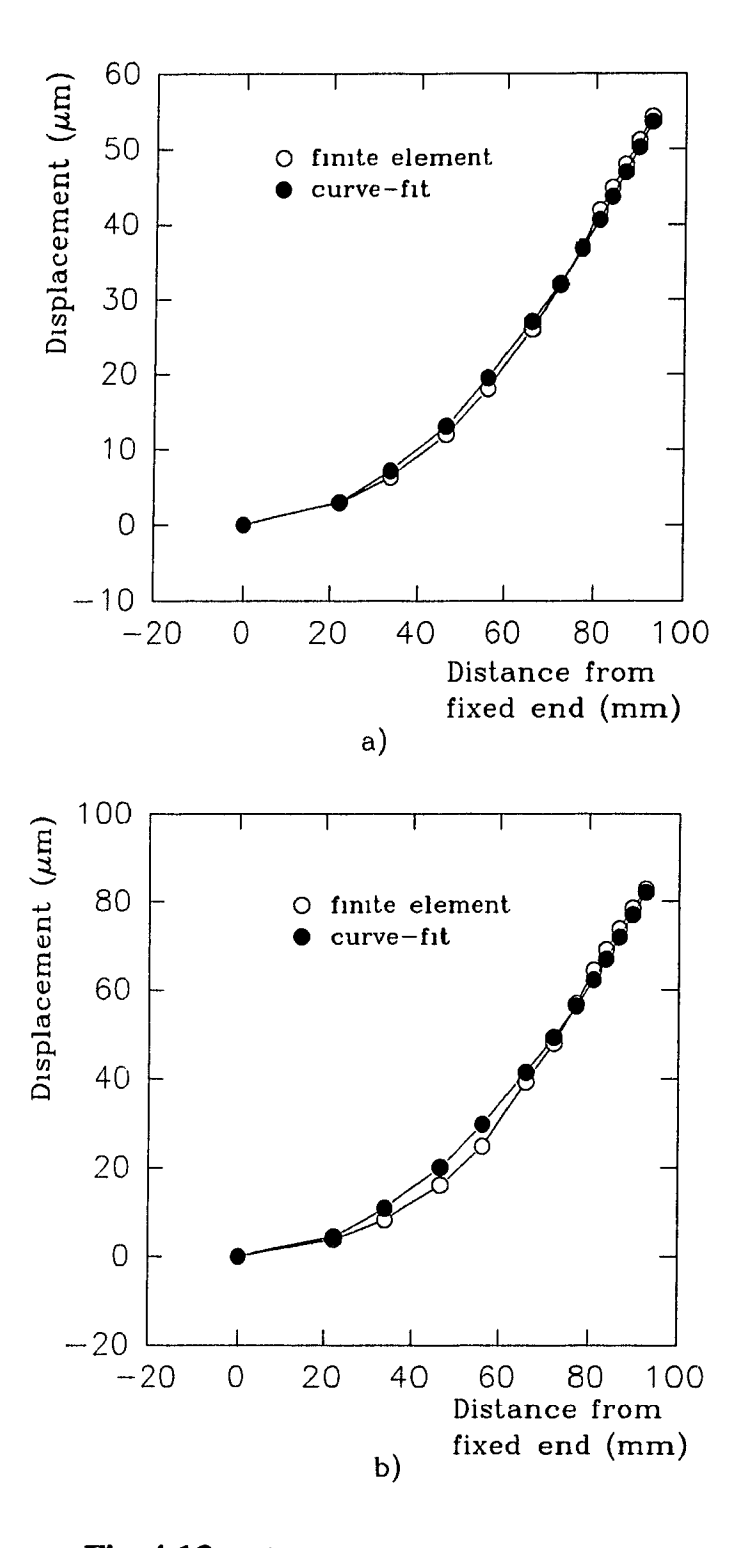


Fig. 4.13 Displacements of nodes along tibial axis.

a) x-direction
b) y-direction

the predictions of relative displacements of the human resurfaced tibia. Nevertheless, it can be used adequately for comparative studies of different fixation models.

# CHAPTER 5

### EXPERIMENTAL METHOD AND RESULTS

#### 5.1 INTRODUCTION

To substantiate the predictions of the finite element analysis of relative displacements at the tibia-prosthesis interface for both the screw and press-fit fixations, and also to provide an experimental comparison between these methods of fixations, an experimental study was performed.

The experimental method of evaluation of the relative displacement at the tibiaprosthesis interface is described in this chapter. An optical method (photomicrography)
was used for measuring the relative displacement in this study. The photomicrographical
technique has been previously used for measuring relative displacement at the interface
[5,18,19]; however, in this study, this technique has been improved by using a
microscope objective of higher magnification (higher resolving power) and by the
employment of a high resolution video camera and an advanced image analysis software.
These improvements allowed more accurate and convenient measurement.

In Section 2, a general description of the test approach is given. Section 3 presents a description of the loading device, measuring system and of the calibration method of the measuring system. The preparation method for tibial specimens, the test procedure and the variables used in this study are described in Section 4. Finally, Section 5 presents the test results corresponding to press-fit and screw fixation of the tibial prosthesis.

#### 5.2 GENERAL TEST APPROACH

Fresh frozen tibial specimens were prepared by removing all soft-tissue structures and by sectioning the specimens 18 cm from the proximal end. The proximal surface of the specimen was then sectioned to create a horizontal surface, perpendicular to the tibial axis, for prosthesis implantation. Once the prosthesis was implanted, the projecting anterior part of the tibia was removed by a cut in the coronal plane, such that the cut surface was flush with the anterior edge of the prosthesis. Thus, the tibia-prosthesis interface was exposed for the measurement of interface relative displacement. Seven locations at the anterior edge of the prosthesis (corresponding to 7 nodes in the finite element model) were marked by vertical grooves of 0.2 mm width. The specimen (Fig. 5.1a) was then placed in a loading device (Fig. 5.1b) and central and eccentric static compressive loads were applied on the prosthesis. A microscope (Fig. 5.1c) connected to a video camera (Fig. 5.1d) was positioned horizontally in front of the exposed interface, viewing each marker at a time. For each location, two images were taken before and after load application. The images were captured and saved in a computer (Fig. 5.1e), using an image processing software. The software was also employed to measure the relative displacement for each location based on the displacement of random markers in the two images.

#### 5.3 DESCRIPTION OF THE EQUIPMENT

#### LOADING DEVICE

The loading device, shown in Figure 5.2, consisted of a stepping motor, controller (stepping motor driver), inverted jack, load-cell, power supply, and voltmeter. The inverted jack, driven by the stepping motor, was connected to a calibrated load-cell placed between the shaft of the jack and a cylindrical loading bar. A small metal ball was attached to the end of the loading bar to allow application of concentrated loads. The controller, capable of generating both continuous and specified step-by-step signals, was used to govern the stepping motor. The output of the calibrated load-cell was measured by the voltmeter.

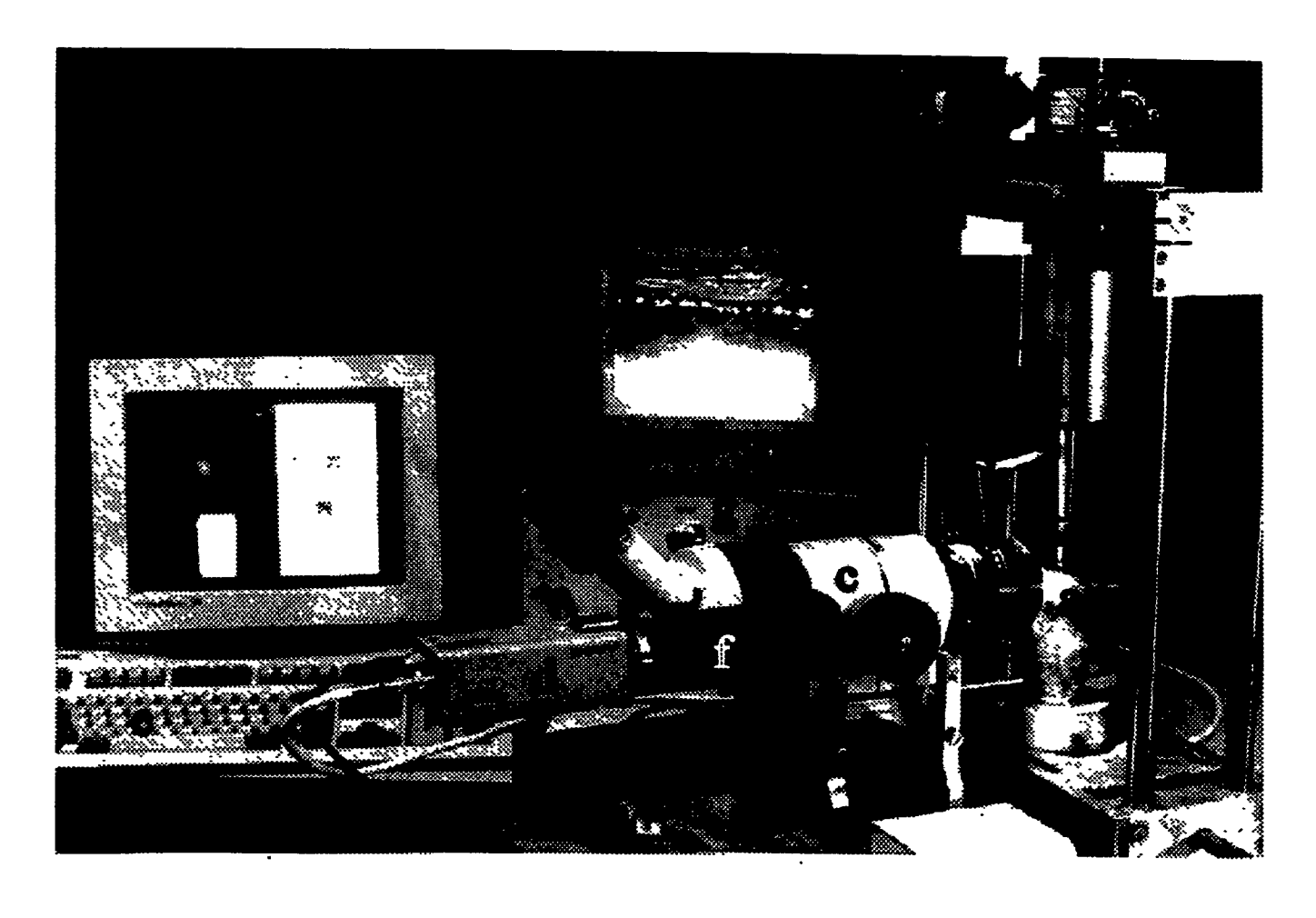


Fig. 5.1 Experimental set-up. a: Specimen, b: Loading device, c: Microscope. d: Video camera, e: Computer, f: Phototube, g. Controller, h Monitor

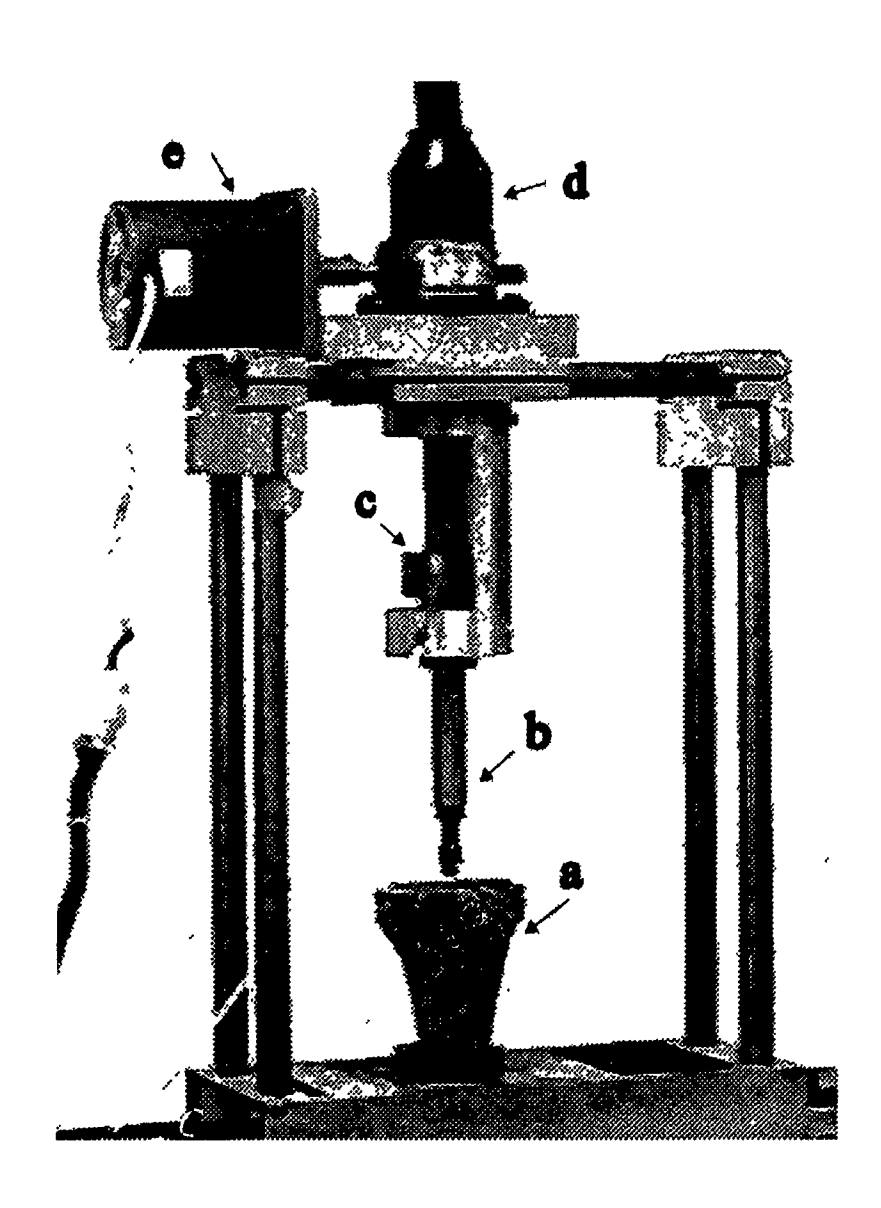


Fig. 5.2 Loading device
a: Specimen
b: Loading bar
c: Load cell
d: Jack
e: Stepping motor

#### **MEASURING SYSTEM**

The measuring system, shown in Figure 5.1, consisted of a CCD (Charged Couple Device) video camera, photo tube, C-mount TV adapter, monochrome monitor, frame grabber board, optical microscope, and an IBM compatible computer. The video camera was connected to the available optical microscope by using the phototube and the TV adapter. The frame grabber board was interfaced with the IBM compatible computer.

The image signals, produced by the camera, were passed through the monochrome monitor displaying the image and were received by the frame grabber board. The frame grabber board, controlled by the image processing software, was used to capture, display and save images as binary files in the computer.

The resolution obtained by this system depended on the magnification set by the microscope. At 80x magnification, the resolution was found to be 1.5  $\mu$ m/pixel.

The characteristics of the different components of the system are described below.

#### 1) The CCD Camera

An AVC-D7 Sony camera was used in the measuring system. This camera is a monochrome video camera which uses a CCD sensor (a solid-state image sensor). The image sensor of this camera with (768 x 493) picture elements produces a high resolution image. Due to the elimination of geometric distortion, it produces precise image geometry. Moreover, photography can be done in a place where the illumination level is very low (minimum illumination: 3 lux with F1.4). Other advantages of this type of camera are its compact size and small weight which allow the camera to be easily used with a microscope.

#### 2) The Stage Micrometer

A stage micrometer was used for the calibration of the measuring system. It consisted of a glass slide (25 x 75 mm) with a scale etched upon it. The scale is 2.2 mm long, with 0.2 mm of the scale divided into 0.01 mm (10  $\mu$ m) divisions; the remaining 2 mm is divided into 0.1 mm intervals.

#### 3) The Microscope

The microscope is the main part of the measuring system. A knowledge of its characteristics is useful for the effective application of the device. The parameters which determine the limitations in using the microscope are described below.

- a) The working distance: This is the distance between the prepared sample and the nearest portion of the objective. An objective with higher magnification, however, requires a lower working distance.
- b) The depth of focus: This is the thickness of the preparation in focus at any one setting of the focusing adjustment. The depth of focus is the most important factor which is determined by the objective; objectives with higher magnification produce a lower depth of focus.
- c) Field of view: This is the diameter of the field of view which depends greatly on the total magnification used.
- d) Resolving power: This is the ability of the microscope to distinguish separate details of closely spaced microscopic structures. This means that if the distance between two lines is smaller than the resolving power of the microscope, they will appear as one line.

The resolving power depends on the objective and the light used to illuminate the specimen. Objectives with higher magnification and light sources with shorter wavelengths provide better resolving power. It is important to note that the eyepiece magnification does not affect the resolving power. The eyepiece only enlarges the details of the prepared sample, resolved by the objective, to be observable to the eye. Under the very best conditions, the naked eye can resolve two points only about 60  $\mu$ m apart [41]. Hence, there is a maximum useful magnification (MUM) for a microscope. Magnification in excess of MUM gives little or no additional resolving power and results in what is termed as "empty magnification".

An optical microscope, the WILD M8 stereomicroscope was used in the measuring system. The depth of focus and working distance were the parameters which limited the use of an objective and/or microscope with higher magnification. By using a special method of preparation of the interface to be described later in this chapter, it

was made possible to use an additional objective of 1.6x which produced a total magnification of 80x. However, the use of this objective reduced the working distance from 87 to 25 mm. This reduction in working distance precluded the use of a ring illuminator, causing a poorer illumination conditions. Also the diameter of the field of view was reduced from 4.2 to 2.6 mm.

#### 4) The Photo Tube and C-Mount TV adapter

A phototube was used to interface the video camera to the microscope. To connect the phototube to the video camera, a C-mount TV adapter was used. However, the disadvantage of the C-mount TV adapter was that it decreased the field of view of the microscope by about 25%.

#### 5) The Frame Grabber

The frame grabber (IP-8, Matrox) was interfaced with an IBM compatible computer. The frame grabber captures and digitizes the image signal output from the video camera and displays them on the Video Graphic Array (VGA) computer monitor. The IP-8 is a grey scale frame grabber and displays 256 grey scale levels or pseudo colours. It has a VGA overlay and single-screen operation features. Its single-screen capability allows it to output the live input signal and the system video signals. Its display resolution varies from (512 x 400) pixels to (1024 x 768) pixels in the non-interlaced and interlaced modes. However, the capturing resolution is (640 x 480) pixels.

#### 6) The Image Processing Software

The Image-Pro Plus package which was used in the measuring system, was chosen to be compatible with the frame grabber board so that it was possible to control the latter directly through the image analyzer software. This eliminated the step of capturing and saving images using the frame grabber driving program. Therefore, for performing different functions from capturing to processing images and measuring, only the image processing software was used. Image processing functions such as contrast

boosting and filtering made it possible to enhance images for convenient measurement.

#### CALIBRATION

The 10  $\mu$ m-division stage micrometer was used for calibration. The image of the scale was taken at the desired magnification and was introduced to Image-Pro Plus as the reference length. By default, Image-Pro Plus displays measurements in terms of pixel. By using the length of the scale as an input, the program calculates the pixels per unit length and displays the measurements accordingly. The calibration is valid only for the adjusted magnification used to image the scale.

#### **5.4 EXPERIMENTAL METHOD**

#### SPECIMEN PREPARATION

A total of six specimens were used in the experiments. After cleaning of the tibial bone specimen by removing all soft-tissue structures, it was cut approximately 18 cm from the proximal end. In order to make a flat surface at the epiphysis, perpendicular to the longitudinal axis of the tibia, the specimen was placed into a short cylinder from the distal end and held firmly in place by three screws installed at three locations around the cylinder. By adjusting the screws, it was attempted to ensure that the tibial axis was parallel to the axis of the cylinder. While the tibia together with the cylinder was held in a clamp, transverse layers were cut at the proximal end of the tibia by a band saw, creating a plateau perpendicular to the tibial axis. Several layers were cut until no subchondral bone remained at the tibial plateau.

The specimen was then removed from the pipe and set in a cylindrical pot, leaving 93 mm of the proximal end of the tibia (the length of the tibia in the finite element model) outside of the pot. The specimen was aligned such that the flat surface was perpendicular to the axis of the pot. While aligned, it was fixed in the pot with fibre glass resin. Since this material shrinks after solidification, six screws were installed in the cylinder walls and the cortical bone, interfacing with the resin, to avoid loosening of the tibial specimen.

After solidification of the resin, the specimen was prepared for implantation of the prosthesis (Fig. 5.3). In order to drill holes in accurate locations, a custom-made jig was used. The jig consisted of a plate with four holes corresponding to the pegs of the prosthesis. Three pins were used to pass through these holes and insert into the bone, holding the jig in place. After the drilling of each hole, a pin was inserted into the hole. Having drilled the holes, the pins and jig were removed and the prosthesis was inserted into place by careful hammering. The diameters of the drill, pin and the peg were chosen to be 7.3, 7.7 and 8 mm respectively.

For screwed prostheses, the prosthesis itself, which was a plate with four holes, was used as a jig. The drill diameter in this case was chosen to be 3.5 mm which was the minor diameter of the screw. The screws were self-tapping and were tightened using a torquerneter such that the final torque was 0.576 N.m (5 lb.in). This is the same torque magnitude that was also used in the finite element analysis of the screw fixation. As explained in Chapter 3, this magnitude of torque was obtained by performing a preliminary test on one specimen.

After implantation, a surface (perpendicular to the tibial plateau) at the anterior edge of the prosthesis was created by a cut in the coronal plane. Special care was taken to have the surface flush with the edge of the prosthesis. The interspace of the trabeculae at this surface was filled with wood glue mixed with a very small amount of aluminium nitride. The aluminium nitride particles appeared as bright spots in photographs and were used as random markers. The use of wood glue had two advantages: first, it helped to make the exposed surface flush with the edge of the prosthesis which, in turn, facilitated the use of objective lenses with higher magnification and, consequently, yielded higher resolution for the measuring system; second, it prevented breakage of the trabeculae.

The screwed and pegged prostheses were fabricated from steel. The pegged prosthesis was made by press-fitting of four pegs (12 mm long, 8 mm diameter) into the steel plate (symmetrical to its two major axes). The screwed prosthesis was simply a steel plate with four holes of 6.5 mm in diameter. Four standard cancellous screws, 30 mm long and 6.5 mm in diameter were used for the screwed prosthesis. The dimensions of



Fig. 5.3 A typical tibial specimen prepared for implantation.

the prosthesis were selected to be 40 mm x 67 mm x 3.5 mm (corresponding to those of the finite element model).

#### TEST PROCEDURE

After preparation of the tibial specimen and implantation of the prosthesis, the specimen was placed in a loading device. Before any measurement, a static central load of 1000 N was applied and repeated ten times for the "conditioning" of the specimen. Before load application, the images of predetermined locations (markers) at the interface were taken and saved in a computer. Load was then applied to the centre of the prosthesis and another set of images of the same locations were captured and saved. The two corresponding images of each location were then displayed on the computer monitor and enhanced for measurement, using the image processing software. This was done using enhancing tools such as contrast boosting and filtering available in the software. Identical markers on the two images were identified and vertical lines were passed through the centre of the markers and the distance between the two lines were measured. The change in distance between the two lines in the two images was considered as the relative displacement at that point. Figure 5.4 shows enhanced images with identified markers.

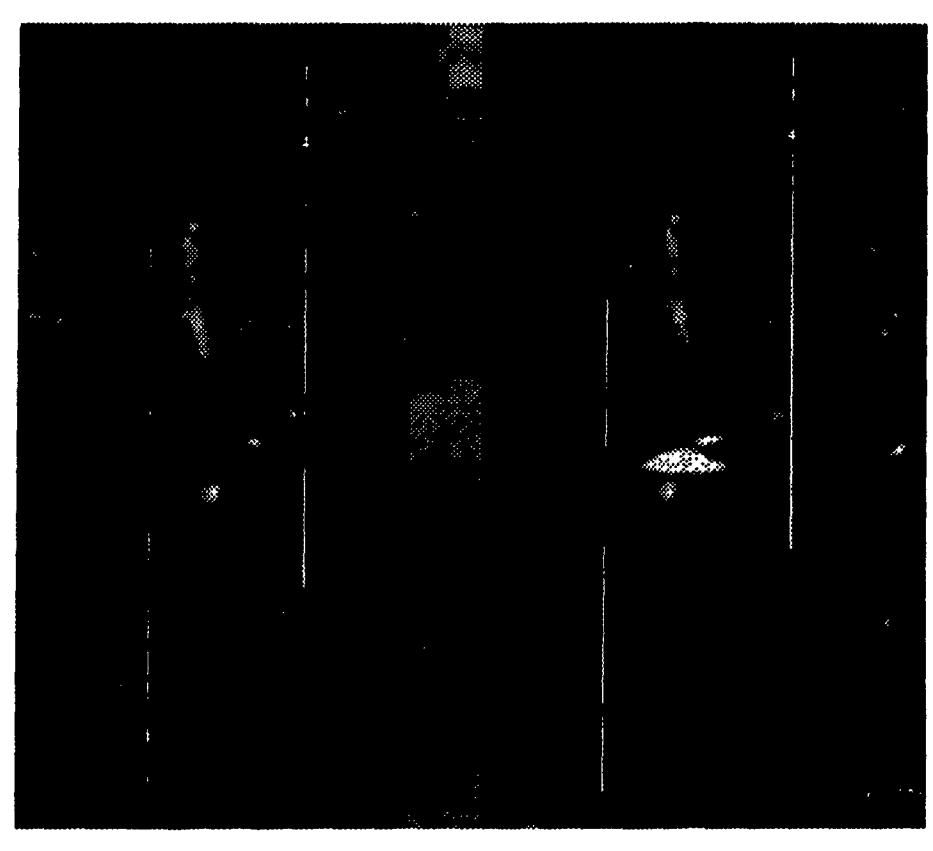
#### **VARIABLES**

Two types of fixation were tested: press-fit and screw fixation. Three specimens were used to test press-fit fixation and three specimens were tested for both screw and press-fit fixations. For the latter three specimens, first the screwed prosthesis and then the press-fitted prosthesis were inserted and tested.

A concentrated load of 1000 N, which was used in the finite element analysis, was applied to the centre of the prosthesis.

#### 5.5 RESULTS

In this section, in addition to the presentation of experimental results, a



a) before load application

b) after load application

Fig. 5.4 Photomicrographic images of a typical location at the horizontal interface before and after load application.

comparison between the latter and the corresponding finite element predictions is provided. Further discussion of the finite element and experimental results is given in Chapter 6.

#### SIGN CONVENTION

In order for consistency in the presentation of the finite element predictions and experimental measurements, the following convention is used. Points 1 and 7, shown in the figure below, represent the lateral and medial side respectively. The prosthesis is considered as the reference and the displacement of the bone with respect to the prosthesis in the medial direction is assumed to be positive.

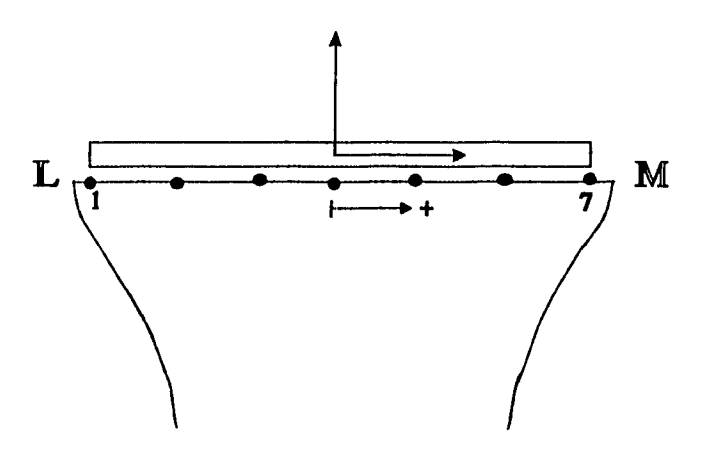


Fig. 5.5 Pictorial representation of the sign convention used in presenting the results.

#### REPRODUCIBILITY OF RESULTS

The reproducibility of the results was verified by performing the measurements three separate times on each specimen. These measurements were carried out under a central load of 1000 N and typical results are shown in Figure 5.6. It is seen that the differences between the three measurements varies for different locations along the interface. The maximum percentage difference between the mean and the results at each location, along the interface, varies from zero (Point 4) to 42% (Point 5), with an

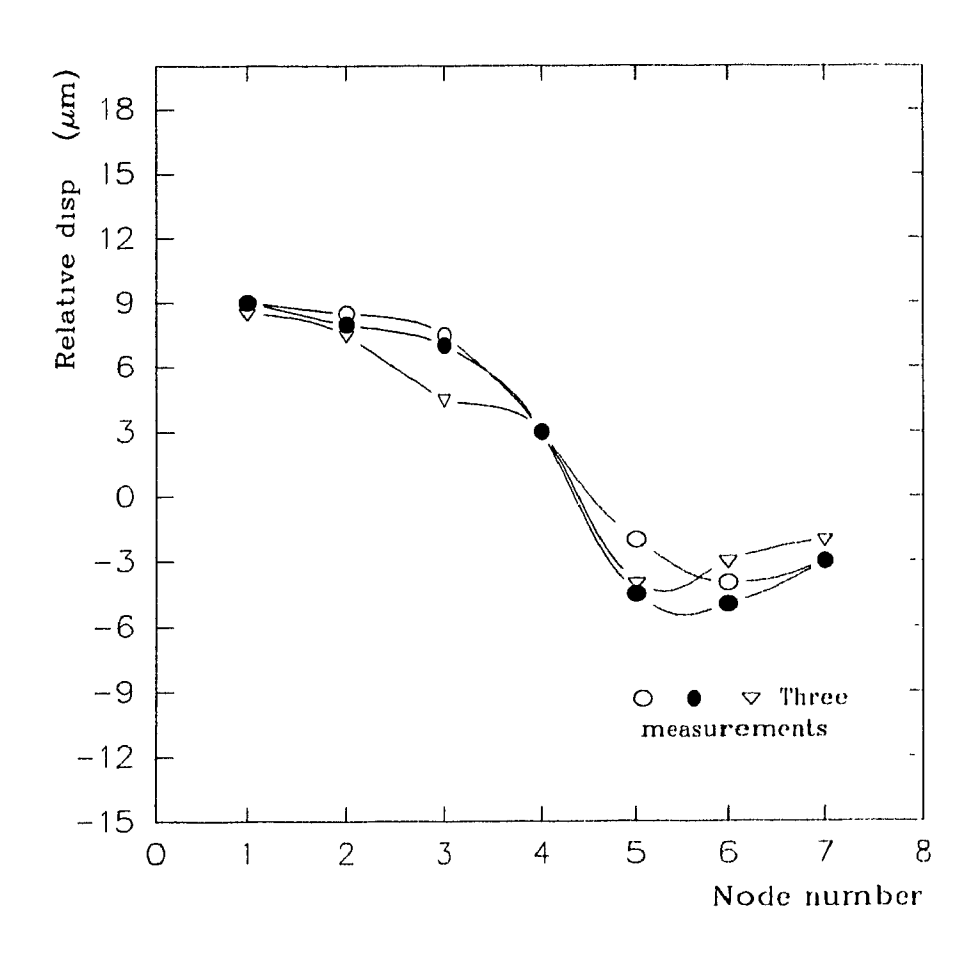


Fig. 5.6 Typical results of three separate measurements of interface relative displacement in x-direction for one specimen with pegged prosthesis.

average of 18%. However, the maximum absolute difference between the results at each location is only slightly larger than the resolution of the measuring system (i.e.  $1.5 \mu m$ ). In view of the small magnitude of the measured relative displacement relative to the resolution of the measuring system, the rather high percentage difference is understandable.

#### **ERROR ANALYSIS**

The measurements were susceptible to two types of error:

- a) Systematic error: Scale error introduced in the calibration procedure could have affected the results of experiments. As mentioned before, the calibration procedure involved taking the image of a standard reference ruler (stage micrometer) and measuring the length with the image processing software in terms of pixels. The error involved in measuring the reference length was checked by repeating the measurement. Based on these measurements, the error was found to be not more than  $\pm 3\%$ .
- b) Random error: The focusing of the microscope is thought to be a source of random error in the measurements. Departure from flatness of the tibia-prosthesis interface at some locations limited perfect focusing of the microscope, resulting in images in which the markers were not exactly in focus. However, by enhancing the images and considering only the centres of the markers as the reference points for measurements, this error was minimized. It is estimated that in the procedure of locating the markers on the computer screen, an error of one pixel which is equal to 1.5  $\mu$ m could have occurred.

#### INTERFACE RELATIVE DISPLACEMENT

Each data point in the plots of measured relative displacement as a function of interface location presented in this section is an average of three separate measurements.

#### Press-Fit Fixation

Press-fit fixation was tested on all six specimens. All measurements were

performed under a central load of 1000 N. Due to the failure of fixation of one specimen and occurrence of error in the replacement of the screwed prosthesis by the pegged prosthesis for another specimen, the results of these two specimens are disregarded. The results of measurements on the other 4 specimens and the corresponding finite element predictions are shown in Figure 5.7. The results of these four specimens show that the relative displacement along the medio-lateral direction does not follow the same pattern for the four specimens. The plots of Specimens 1 and 2 have relatively similar patterns with a small difference in magnitudes of the relative displacement. Both plots are completely in the positive zone which implies that all points at the bone side of the interface have displacements in the medial direction with respect to the prosthesis. The plot of Specimen 3 shows relatively a similar pattern with that of Specimen 1; however, the magnitudes of the relative displacements are higher than those of Specimen 1 and lie both in the positive and negative zones. The plot of Specimen 4 shows a completely opposite pattern with those of the first three specimens but with magnitudes closer to those of specimen 3.

The difference in the pattern of the results for the four specimens is due likely to the location of the load relative to the neutral axis of the tibia for each specimen. During prosthesis implantation, due to uncertainty in the location of the neutral axis, it was not possible to ensure conformity of the centre of the prosthesis with the neutral axis of the tibial specimen. Hence, some eccentricity of the prosthesis centre relative to the neutral axis of the tibia must be expected. In this case, the application of the load, although at the centre of the prosthesis, produced bending moments in the lateral or medial directions and consequently affected the pattern of distribution of the relative displacement.

In Figure 5.7 the measured relative displacements are also compared with the predictions of the finite element analysis. It is seen that the pattern of relative displacements is relatively similar to those of three of the specimens and is dissimilar to that of one. Once again, the position of the load relative to the neutral axis of the tibia is likely the source of discrepancies between the pattern of finite element predictions and the experimental measurements. In addition to the differences in pattern, the maximum

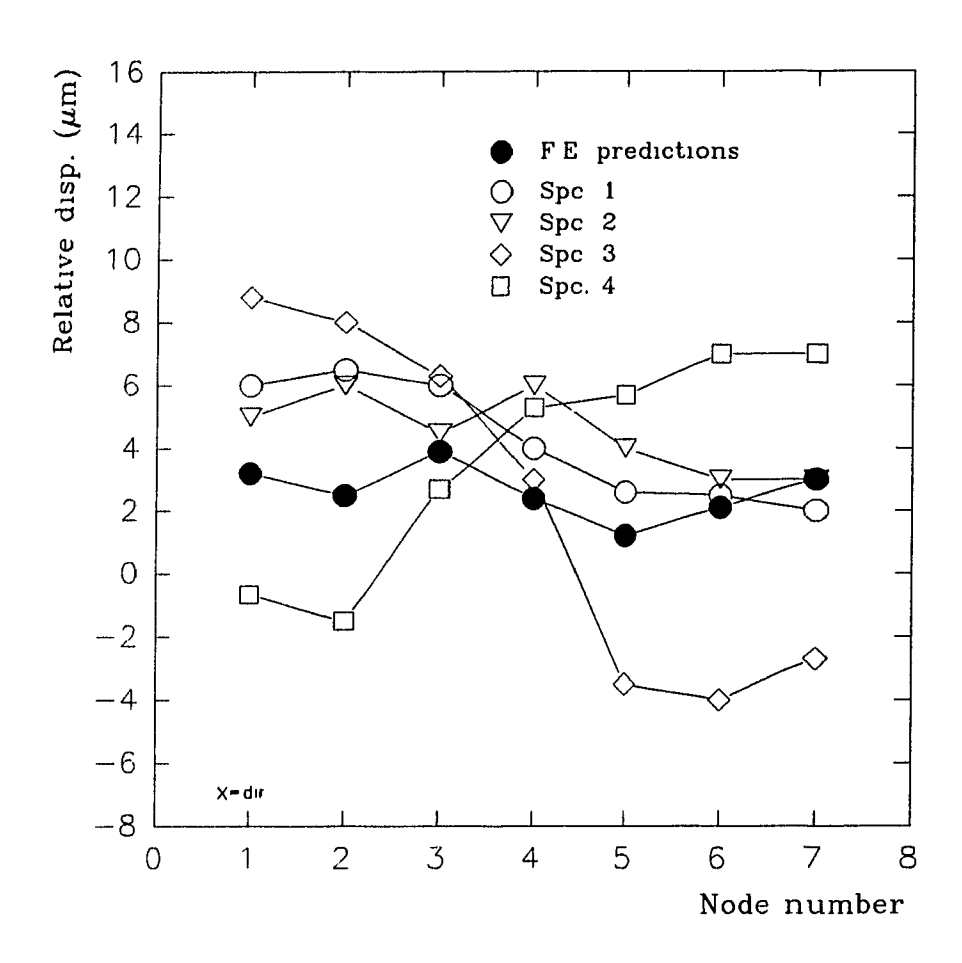


Fig. 5.7 Comparison of the finite element results of the interface relative displacement and measurements for the press-fit fixation.

relative displacement predicted by the finite element analysis is only 3.9  $\mu$ m, which is smaller than those measured in all four specimens (i.e. 6, 6.5, 7, and 9  $\mu$ m).

#### Screw Fixation

For the last three specimens, both the screw and the press-fit fixations were tested. Therefore two comparisons can be made for the results of these three specimens: comparison of the finite element predictions and the experimental results and a comparison between the experimental results of the screw and the press-fit fixations. The former comparison was made previously for the press-fit fixation (refer to Fig. 5.7). A comparison of the experimental results and the corresponding finite element predictions for the screw fixation is shown in Figure 5.8. Both finite element predictions and experimental results show that for the screw fixation the relative displacements are very small. The measurements are approximately of the same magnitude as the resolution of the measuring system (i.e.  $1.5 \mu m$ ). The maximum relative displacement predicted by the finite element analysis and measured in the experiment is about  $3 \mu m$ .

The experimental results of the screw and the press-fit fixations are compared in Figure 5.9. Since the measurements for the press-fit fixation for one of these specimens were disregarded (as explained before), the experimental comparison of the screw and the press-fit fixations has been made for only two specimens. The results of both specimens show that the screw fixation significantly reduces the interface relative displacements in comparison with the press-fit fixation. The average measured relative displacements for the screw fixation are 1 and 2  $\mu$ m and those for the press-fit fixation are 4.2 and 4.5  $\mu$ m for the two specimens.

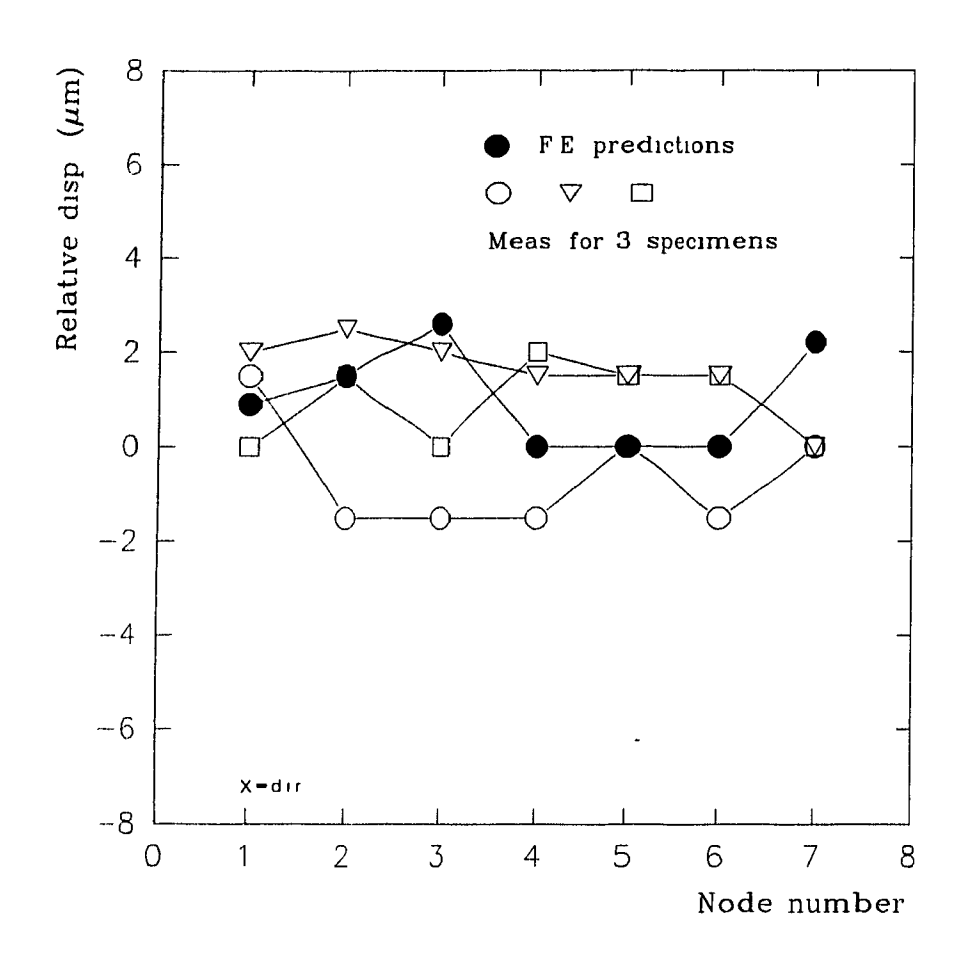
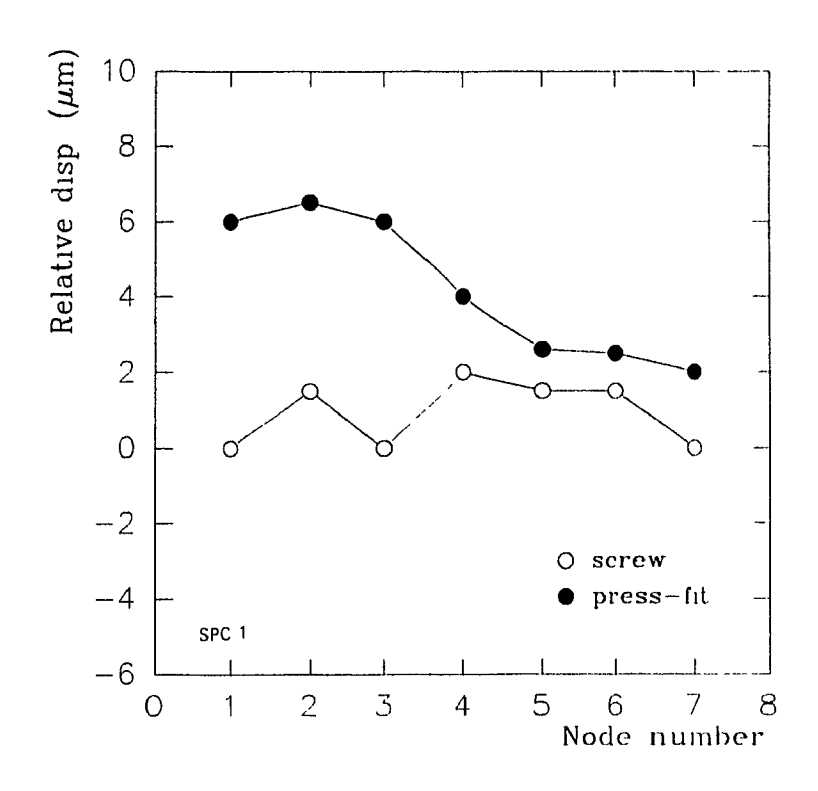


Fig. 5.8 Comparison of the finite element results of the interface relative displacement and measurements for the screw fixation.



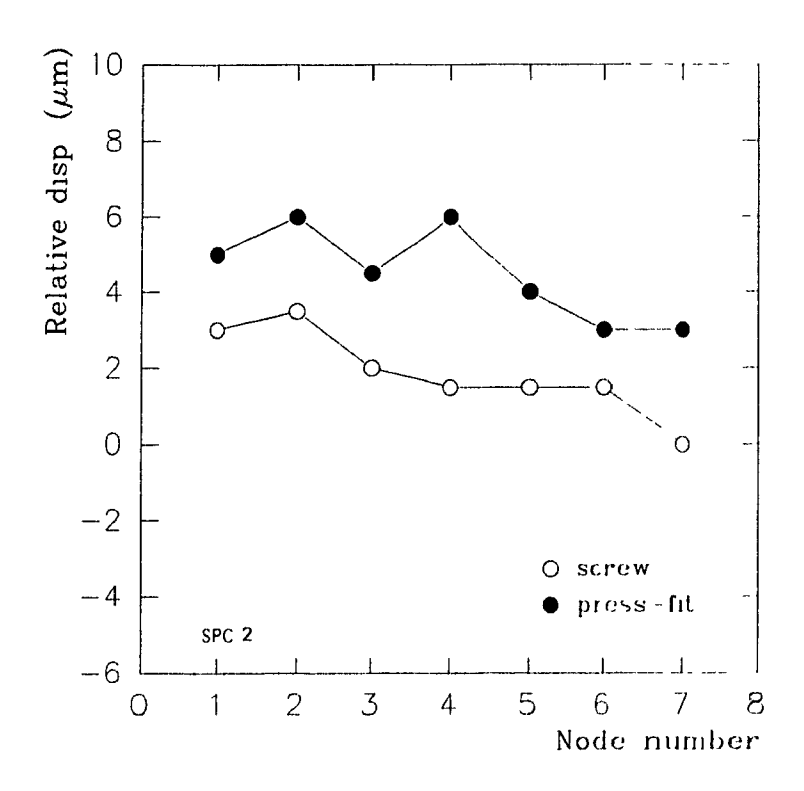


Fig. 5.9 Comparison of experimental results for the press-fit and the screw fixations.

# CHAPTER 6

### **DISCUSSION OF RESULTS**

In this chapter, the finite element and experimental results which were presented in Chapters 4 and 5, are discussed. First, limitations which might have affected the results are presented. Then results of finite element analysis and experimental measurements for the two types of fixation are compared. Finally, a comparison of results with those of previous studies is attempted followed by a presentation of clinical implications.

#### 6.1 LIMITATIONS OF THE STUDY

#### FINITE ELEMENT MODEL

In the finite element model, cancellous and cortical bone materials were assumed to be linear, isotropic, but inhomogeneous. For the analyses in which the external load is in the direction of the longitudinal axis of the bone and in the range of normal physiological loading, the simplifying assumptions of linear and isotropic material for bone has been shown to have little effect on the results [36]. Inhomogeneity of bone materials was partially taken into account by assigning 25 different elastic moduli to cancellous and cortical bones. However, these elastic moduli were average values as reported in the literature [29] and might have differed from those of the specimens used in the experiment.

Geometry of the finite element model of the tibia was determined based on dimensional data measured from a tibial specimen of average size. There were differences, both in size and shape, between the model and the specimens used in the experiment.

The material properties and geometry of the model are believed to be the major sources of discrepancies between the results of the finite element analysis and experimental measurements.

Finite element analysis of models involving contact of bodies introduces an additional parameter, which is the friction between contact surfaces. Frictional properties of contact surfaces could constitute another source of discrepancy between finite element results and measurements of the physical model. The difference between frictional properties assigned to the model and the actual values in the physical model can be significant when contact occurs with bone. Like the other properties of bone, frictional properties vary widely. Furthermore, irregularities at the horizontal interface caused by the cutting of the bone, is also likely to affect the frictional properties. Therefore, unless the coefficient of friction is measured for each specimen used in the experiment, the coefficient of friction taken from the literature can only be an approximation.

#### MAGNITUDE OF THE RELATIVE DISPLACEMENT

In this study, measurements at the peg-hole interface were not performed due to the lack of access to this interface. However, the finite element findings of both the close-fit and press-fit models demonstrate that the maximum relative displacement along the pegs is less than the maximum relative displacement at the horizontal interface (for the case where the length of the peg is equal to the depth of the hole).

In general, both the finite element and experimental magnitudes of interface relative displacements obtained in this study, are much less than 150  $\mu$ m which is known to be the upper bound for the possibility of bone ingrowth [42]. The maximum relative displacement found in this study is about 9  $\mu$ m which was measured for a central compressive load of 1000 N. However, it should be noted that the relative displacements

obtained in this study are not representative of those occurring in actual resurfaced tibiae because of the following reasons:

1- The length of the tibia. In the experiment and the finite element model only a proximal portion of the tibia is considered. As demonstrated by the finite element results in Chapter 4, the relative displacement at the interface vary with approximately the square of the length of the tibia. The effect of the length of the tibia on the relative displacement is the parameter which was generally neglected in previous studies.

2- Loading conditions. As stated in Chapter 2, the magnitude of physiological forces acting between the tibia and femur (joint-contact forces) ranges from two to seven times body weight for normal activities, while the magnitude of the force used in this analysis (i.e. 1000 N) was only approximately 1.5 times body weight. Additionally, these forces are not necessarily collinear with the tibial axis.

However, evaluation of the actual interface relative displacements of the resurfaced tibia was not the goal of this study. As far as comparison of different fixation methods is concerned, the length of the tibia considered in the analysis is not expected to play a major role.

#### PARAMETERS INFLUENCING THE EXPERIMENTAL RESULTS

Various factors influenced the experimental results, causing the difference with the finite element results. These factors can basically be classified into two categories.

1- Parameters related to the characteristics of the tibia. These are material and frictional properties, and geometry whose variability is significant. In addition to these, the porous structure of the cancellous bone, which is formed by trabeculae, introduces an uncertainty in the measured relative displacement at the interface. Since the cancellous bone is not a continuous material even at a macroscopic scale, one cannot assure that no local deformation of trabeculae adjacent to the prosthesis occurs. The assumption of local deformation of the trabeculae being independent of the overall deformation of the specimen, implies that there would be some errors in the measured relative displacement. However, in this experiment, a low elastic-modulus material (e.g. wood glue) was used

to fill the inter-trabecular space of the exposed surface. It is believed that this material improved the chances of preventing local deformation and breakage of the trabeculae. This material, which is applied only sparingly to the exposed surface of the bone, would have insignificant effect on the overall stiffness of the proximal tibia.

- 2- Parameters related to the specimen preparation. Five parameters are of concern:
- a) Relative position of the prosthesis centre and the tibial axis: Since the load is applied at the centre of the prosthesis, the load could vary from a purely compressive force to a combination of compressive force and bending moment depending on the relative location of the prosthesis centre with respect to the tibial axis;
- b) Flatness of the horizontal interface: This cutting-related parameter affects the results in two ways: i) by changing the distribution of the load (due to non-flatness, random locations come in contact and load is transmitted only through these contact areas); ii) by changing the frictional properties (the frictional properties are dependent on the degree of irregularities at the horizontal interface);
- c) Relative position and the diameter of the hole and peg: This parameter can be the source of rigid body motion of the prosthesis with respect to the underlying bone. However, this factor was minimized by using a jig in order to have holes in accurate relative positions and using a smaller diameter drill for drilling holes;
- d) Depth-of-cut: In order to prepare the tibial plateau for prosthesis insertion, a portion of the bone at proximal tibia needed to be resected. The depth-of-cut determines the strength of the bone adjacent to the interface which, in turn, affects the relative displacement at the interface. The smaller is the depth-of-cut, the higher will be the strength of the bone adjacent to the interface.
- e) Relative alignment of the angle between the horizontal interface, the tibial axis and the load direction: Poor alignment, for instance, could produce an undesirable tangential component along the horizontal interface from an axial load.

Among these parameters (a) and (b) are more difficult to control. All of the above parameters can be considered as potential sources of discrepancies between the finite

element and experimental results. In fact, it would be difficult to take into account all of these parameters in any one finite element model

## 6.2 COMPARISON OF FINITE ELEMENT AND EXPERIMENTAL RESULTS PRESS-FIT FIXATION

The finite element results show that the press-fit fixation is not necessarily preferable to the close-fit fixation in as far as the reduction of the relative displacement at the horizontal interface is concerned. In the press-fit fixation case, relative to the close-fit situation, although the relative displacement decreases in the medio-lateral direction, it increases in the anterior-posterior direction (Chapter 4, Fig. 4.7). The total relative displacement (summation of the relative displacements in the medio-lateral and anterior-posterior directions) for the press-fit fixation model is larger than that for the close-fit model. Comparison of the contact forces show that for the press-fit fixation model, the normal contact forces at the horizontal interface are smaller than those for the close-fit model (Chapter 4, Fig. 49). These results substantiate the predicted increase in the relative displacement at the horizontal interface. Since the normal contact forces are only compressive, reduction of the contact forces at the horizontal interface causes a decrease in the frictional forces, yielding an increase in the relative displacement at the interface. Therefore, this finite element result appears to be at variance with the idea of press-fitting of pegged prosthesis for the purpose of reducing the relative displacement at the bone-prosthesis interface (as opposed to close-fitting).

The contact pressures at the peg-hole interface, predicted by the finite element analysis are in good agreement with those obtained by closed-form solution (refer to Chapter 4, Fig. 49). But both finite element modelling and closed-form solution for press-fit situations are based on the fact that all interference is transformed to elastic deformation, which causes compressive stresses at the interface. This condition can be achieved only through the classical method of press-fitting of mechanical parts in which, the diameter of the female part is enlarged by increasing its temperature. This provides easy insertion of the male part without any damage. After cooling, both components

experience elastic deformation which causes compressive stresses at the interface. In such a state, the press-fit can be modelled by the finite element method as explained in Chapter 3.

In the present case, however, a prosthesis is forcefully fitted into the tibia. Therefore, local damage to the peripheral bone in the peg hole would occur. Such damage was noted during the experiment. A drill of 7.3 mm diameter was used to make the holes. By inserting the pins of the jig into the bone, which was used to accurately locate the relative positions of the holes, the diameters of the holes were enlarged to the pin diameter of 7.7 mm. The prosthesis had pegs of 8 mm diameter, therefore, there was an interference of 0.3 mm (about 4% of the peg diameter). After inserting the prosthesis and performing the tests, the prosthesis was removed and the diameters of the holes were measured. The results showed the diameters to have increased to 8 mm, the same as that of the pegs. Therefore, after removal of the prosthesis, the 0.5 mm interference was not recovered at the bone side and, evidently, was destroyed during the prosthesis insertion.

In addition, for the pegged prosthesis, press-fitting with an interference of 5% of peg diameter (that is commonly used for press-fitting of pegged prostheses) theoretically yields compressive stresses at the peg-hole interface of about 11.5 MPa. This was obtained by using Equation 3.4 and assuming the interference causes only elastic deformation of the bone without damage. Goldstein *et al.* [29] reported the ultimate strength of cancellous bone at the proximal tibia to be as low as 1 MPa, and as high as 12 MPa at load bearing regions. Therefore, the stresses due to a 5% interference (11.5 MPa) are likely to cause failure of the bone.

In conclusion, although interference in the press-fit case is useful for compensating any inaccuracies in the drilling of the holes (which could occur in position, diameter or angle between the longitudinal axis of the hole and the plane of horizontal interface) the press-fit conditions are not achievable by the technique used for the implantation of pegged prosthesis. This technique yields a fixation which resembles more a close-fit fixation than a press-fit one. That is to say, the finite element model of the press-fit fixation of the prosthesis into bone is not realistic. Therefore, the experimental

results of the pegged prosthesis should be compared with the finite element results for the close-fit fixation model.

Although in Chapter 5 (Fig. 5.7) the experimental results of pegged prosthesis were compared with the finite element results for the press-fit model, here the same comparison is valid for the measurements and the finite element results of close-fit model. This is because the finite element results for both the close-fit and press-fit models follow the same pattern (except for one point as seen in Fig. 6.1) and in addition, the differences in magnitudes are small in comparison to differences of these results with the measurements. The sources of discrepancies between the finite element results and measurements are believed to be due mainly to the material and frictional properties and the implantation procedure, as explained in Section 6.1.

#### **SCREW FIXATION**

The effect of the screw fixation in preventing separation of the tibit and prosthesis at the horizontal interface was not considered in the finite element model. This effect is due to the interlocking of the screw teeth with the bone which constrains the relative displacement between the screw and the bone in the z-direction (along the screw axis). However, it has to be noted that in the case of screw fixation, separation occurs due only to large eccentric loads. Therefore, under a central load, the elimination of the effect of the screws in preventing separation, would have an insignificant effect on the results

The superior performance of screw fixation with respect to press-fit fixation in the reduction of the relative displacement at the horizontal interface was consistent for all the tibial specimens tested both for screw and press-fit fixations. On average, the experimental results show that the screw fixation causes a decrease in the relative displacement by about 76% with respect to the press-fit fixation. The important point to be noted here is that screwed and pegged prosthesis were tested on the same specimen. Therefore many parameters which could cause uncertainties in the comparison were eliminated.

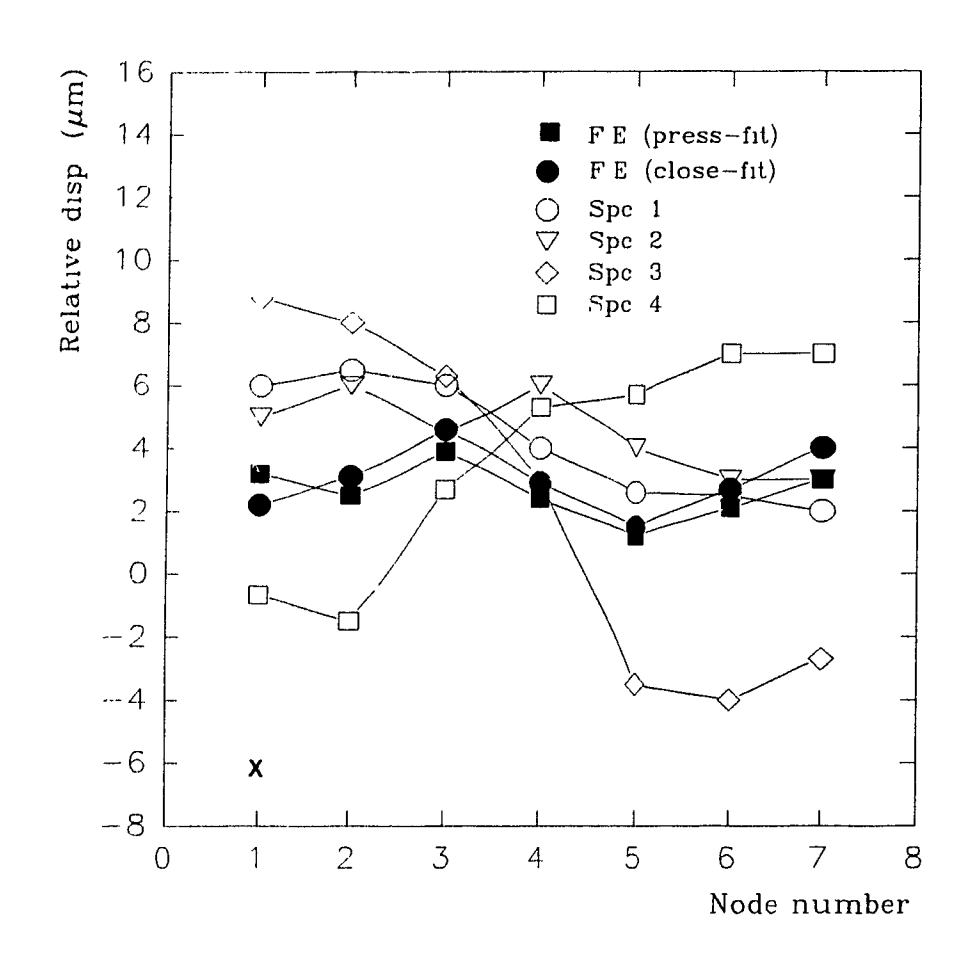


Fig. 6.1 Comparison of the finite element results for the press-fit and the close-fit models and measurements for pegged prosthesis.

The advantage of the screw fixation over the press-fit fixation was also predicted by the finite element analysis. The finite element modelling of the screw fixation was based on the effect of a tightened screw in introducing initial compressive torces at the horizontal interface of the bone and prosthesis. Based on the tightening torque it was calculated that each tightened screw introduces a significant initial compressive force of about 220 N (approximately 1/3 of body weight) on to the prosthesis which, in turn, causes frictional forces against the relative displacement at the interface. The finite element results show that screw fixation decreases the relative displacement at the interface by 65% with respect to press-fit fixation.

#### **6.3 COMPARISON WITH PREVIOUS STUDIES**

In a finite element stress analysis of the press-fit fixation of the tibial prosthesis, using an axisymmetric model with gap elements at the interface, Dawson *et al* [6] found that press-fitting of the pegs reduces the compressive stresses at the horizontal interface. This is in agreement with the reduction of contact forces at the horizontal interface for the press-fit fixation found in the present study.

Among the finite element analyses which have evaluated interface relative displacement for a prosthesis with pegs, the analysis performed by Tissakht *et al* [5] is the closest one to the present study. In their analysis, a two-pegged prosthesis with no friction at the interface was modelled. The authors obtained relative displacements at the outer edge of the prosthesis of magnitude up to 27  $\mu$ m for a central load of 1000 N. In this study, which uses a four-pegged prosthesis and considers interface friction, a maximum relative displacement at the same region was found to be only 8  $\mu$ m. The large difference between the results of the two studies is due to the differences in material properties, consideration of friction and the number of pegs of the prosthesis.

For the screw fixation, there is no previous finite element analysis which has

modelled the screw fixation. However, there have been several experimental studies which were concerned with the comparison of the screw and press-fit fixations [10,12,15,16]. Due to differences in experimental methods, prosthesis configurations, loading conditions, and specimens used in these experiments; a quantitative comparison between previous experiments and the present study is difficult. However, in these experimental studies it has been demonstrated that the screw fixation significantly reduces the relative displacement in comparison with the press-fit fixation. For example, Strickland *et al.* [16] has reported that the relative displacement for prostheses with screws is about one-third of those for prostheses with only pegs.

#### 6.4 CLINICAL IMPLICATIONS

Both the finite element and experimental results strongly substantiate the use of screws for initial fixation of prosthesis. A large compressive force introduced at the interface by screws significantly reduces the relative displacement. The effect of screws in introducing a compressive force at the interface is due to the tightening torque. A larger tightening torque yields a larger compressive force at the interface. Therefore, screws have to be used in denser regions of the tibial plateau so that larger magnitudes of torque could be applied. This can be extended to the use of longer screws which pass through the cancellous bone, and engage with the cortical shell.

Although the finite element analyses predicted that the relative displacements for the press-fit model are larger than those for the close-fit model, the consideration of the interference is recommended for the implantation of pegged prostheses. The interference does not provide the press-fitting conditions at the peg-hole interface as was explained earlier in this chapter; however, it does compensate for inaccuracies which could occur in the implantation procedure (drilling of holes).

# CHAPTER 7

## SUMMARY OF CONCLUSIONS

#### 7.1 INTRODUCTION

As was mentioned in Chapter 1, this study was planned to provide a comparison of performance of the two fixation methods (i.e. screw and press-fit fixations) in reducing relative displacement at the tibia-prosthesis interface, using both finite element analysis and measurement.

New approaches for the analysis of fixation methods were attempted and the findings were discussed in detail in previous chapters. The important conclusions of this work accompanied by some proposals for further research are presented in this chapter

#### 7.2 SUMMARY OF CONCLUSIONS

The finite element analysis of the press-fit model demonstrated that this type of fixation is not preferable to close-fit fixation for the reduction of the relative displacement at the horizontal interface; however, at the peg-hole interface the results exhibit a decrease in the relative displacement for the press-fit model. The prediction of finite element analysis have been found to be consistent with the results of closed-form analysis

in terms of predicting the contact pressure at the peg-hole interface. However, based on experimental observations it is believed that the press-fit conditions are not achievable during actual implantation because of bone damage. Nonetheless peg-hole interference is useful for compensating maccuracies in the implantation (surgical) procedure.

For the first time, modelling of screw fixation using the finite element method has been performed. The effect of screws in providing significant initial compressive forces at the horizontal bone-prosthesis interface has been considered in the finite element model. The finite element results show that screw fixation causes a significant decrease in the relative displacement at the horizontal interface. The measurement of relative displacements also clearly reveal that screw fixation relative to press-fit fixation reduces the relative displacement at the horizontal interface.

The results of the finite element analysis show that consideration of friction at the bone-prosthesis interface has a significant effect on the relative displacement. Hence, it is deemed essential that frictional properties be considered in the finite element modelling of fixation methods. In fact, modelling of cementless fixations without taking into account friction is considered to be unrealistic.

It has been observed that measurements of interface relative displacements are affected by a number of parameters. These are related to: tibial characteristics, such as material and frictional properties and geometry; and the specimen preparation and implantation procedure. From a clinical point of view, the factors relevant to specimen preparation and implantation procedure can be regarded as those surgical entities which determine the accuracy of implantation and hence, affect the interface relative displacement. From a technical point of view, these parameters can be considered as

potential sources of discrepancies between finite element predictions and experimental results.

#### 7.3 DIRECTIONS FOR FURTHER STUDIES

The finite element modelling of the screw fixation was attempted for the first time. As mentioned before, the experimental results of screw fixation were affected by various parameters such as material and frictional properties and the geometry of the tibial specimen. Since screw fixation is used in connecting various mechanical parts, a separate more general study would be beneficial to a wide range of applications. It is suggested that a finite element model of screw fixations between two parts with a simple geometry and known material and frictional properties be developed. Such a model would eliminate the major factors causing differences between finite element and experimental results, except those related to the method of modelling the screw fixation itself. Therefore, a more accurate verification of the method of modelling the screw fixation can be done.

There are a number of parameters related to the tibial characteristics and specimen preparation and implantation procedure which affect the measurements of interface relative displacements, some of which were described in Chapter 6. However, evaluation of the influences of these parameters was beyond the scope of this work. Further study of the effects of these parameters, especially, of those related to the accuracy of implantation (surgical accuracy) on the interface relative displacement, would be beneficial in clinical applications.

#### REFERENCES

- 1. R. Huiskes and E.Y.S. Chao, "A Survey of Finite Element Analysis in Orthopaedic Biomechanics: The First Decade," *J. Biomechanics*, Vol. 16, No. 6, pp. 385-409, 1983.
- 2. R. Natarajan and T.P. Andriacchi, "The Influence of Displacement Incompatibilities on Bone Ingrowth in Porous Tibial Components," *34th Trans. Orthopaedic Research Society*, pp. 331, 1988.
- 3. R. Natarajan and T.P. Andriacchi, "The Influence of Continuum Assumption on Displacement Incompatibilities in the Porous Implant-Bone Interface," *35th Trans. Orthopaedic Research Society*, pp. 383, 1989.
- 4. A. Shirazi-Adl and A.M Ahmed, "A Parametric Axisymmetric Model Study on the Interface Motions in Porous-Surfaced Tibial Implants," *Annals of Biomedical Engineering*, Vol. 17, pp. 411-421, 1989.
- M. Tissakht, A. M. Ahmed and G. Mulas, "Measurement of Bone/Prosthesis Interface Relative Motion: Comparison With Analytical Predictions," 10th Annual Conf. Canadian Biomaterials Society, pp. 39-42, 1989.
- J.M. Dawson and D.L. Bartel, "Consequences of an Interference Fit on the Fixation of Porous-Coated Tibial Components in Total Knee Replacement," J. Bone and Joint Surgery, Vol. 74-A, No. 2, pp. 233-238, 1992.
- 7. K.G. Nilson, J. Karrholm and L. Ekeleund, "Cemented Versus Uncemented Tibial Component in Tricompartmental Miller-Galante Knee Arthroplasty Due to Gonarthrosis," *37th Trans. Orthopaedic Research Society*, pp. 165, 1991.
- 8. L.V. Carlsson, L. Ryd and p. Herberts, "An In-Vivo Roentgen Stereogrammetric Analysis of the Miller-Galante Tibial Component," *37th Trans. Orthopaedic Research Society*, pp. 168, 1991.
- 9. I. Yoshii, L.A. Whiteside and S.E. White, "The Effect of Material Properties of the Tibial Tray on Micromovement CoCr vs Ti6Al4V," 37th Trans. Orthopaedic

- Research Society, pp. 167, 1991.
- D.R. Sumner, A. Berzins and T.M. Turner, "Stability of the Tibial Tray in Cementless TKA: Initial vs. Late Post-Operative Motion," 38th Trans. Orthopaedic Research Society, pp. 268, 1992.
- H. Shimagaki, J.E. Bechtold, R. Sherman and R.B. Gustilo, "Initial Stability of Tibial Components In Cementless Total Knee Arthroplasty," 34th Trans. Orthopaedic Research Society, pp. 477, 1988.
- 12. A.D. Kaiser and L.A. Whiteside, "Comparison of Screws and Pegs for Initial Fixation Stability in a Unicondylar Knee Prosthesis," *36th Trans. Orthopaedic Research Society*, pp. 474, 1990.
- 13. R.G. Volz and R.W. Lee, "The Effect of the Stem and Stem Length on the Mechanical Stability of Tibial Knee Components," 34th Trans. Orthopaedic Research Society, pp. 472, 1988.
- 14. T.P. Andriacchi, A.B. Strickland and D.R. Sumner, "Mechanical Factors Influencing Ingrowth into the Tibial Component of Total Knee Replacement," *Computational Methods in Bioengineering*, ASME Bed-Vol.9, pp. 135-142, 1988
- 15. H. Miura, L.A. Whiteside, J.C. Easley and D.D. Amador, "Effects of Screws and Sleeve on Initial Fixation in Uncemented Total Knee Tibial Component," *34th Trans. Orthopaedic Research Society*, pp. 474, 1988.
- 16. A.B. Strickland, K.H. Chan, T.P. Andriacchi and J. Miller, "The Initial Fixation of Porous Coated Tibial Components Evaluated by the Study of Rigid Body Motion Under Static Load," *34th Trans. Orthopaedic Research Society*, pp. 476, 1988.
- 17. H. Kambic, B.N. Stulberg, T. Manning, J.T. Watson, "Application of Video-Micro Scaler Technique for the Quantification of Micromotion in a Unicondylar Knee Replacement Model," *38th Trans. Orthopaedic Research Society*, pp. 323, 1992.
- 18. W.C. Kim, D.V. Bass and S.H. Anzel, "Screw Fixation of Tibial Trays: Stability and Strength Assessment Using a High Resolution Video and Instron Machine," 38th Trans. Orthopaedic Research Society, pp. 24, 1992.
- 19. A. Yang, D.R. Sumner, S. Choi, R. Natarajan and T.P. Andriacchi, "Direct

- Measurement of Micromotion at the Bone-Implant Interface: The Tibial Component in a Canine Model," 36th Trans. Orthopaedic Research Society, pp. 233, 1990.
- 20. J.C. Boileau Grant, "An Atlas of Anatomy," The Williams & Wilkins company, Baltimore, pp. 271,293, 1956.
- 21. A.M. Ahmed, "Internal Mechanics of the Human Knee Joint," 6th International conference on biomedical engineering, Singapore, 1990.
- 22. T.M. Wright and A.H. Burstein, *Musculoskeletal Biomechanics*, Surgery of the Musculoskeletal System, Churchil Livingstone, New York, pp. 231-250, 1990.
- 23. P.R. Cavanagh and M.A. Lafortune, "Ground Reaction Forces in Distance Running," *J. Biomechanics*, Vol. 13, 397-406, 1980.
- 24. H. Elftman, "The Forces Exerted by the Ground on Walking," *Arb. Physiology*., Vol. 10, 485, 1939.
- 25. J.B. Morrison, "The Forces Transmitted to the Human Knee Joint During Activity," *Doctoral Thesis*, University of Strathclyde, 1967.
- 26. J.B. Morrison, "The Mechanics of the Knee Joint in Relation to Normal Walking," J. Biomechanics, Vol. 3, pp. 50-61, 1970.
- 27. A. Seireg and R.J. Arvikar, "The Prediction of Muscular Load Sharing and Joint Forces in the Lower Extremities During Walking," *J. Biomechanics*, Vol. 8, pp. 89-102, 1975.
- K.J. Bathe and A. Chaudhary, "A Solution Method For Planar and Axisymmetric Contact Problems," *International Journal for Numerical Methods in Engineering*, Vol. 21,6 pp. 65-88 1985.
- S.A. Goldstein, D.L. Wilson, D.A. Sonstegard and L.S. Matthews, "The Mechanical Properties of Human Tibial Trabecular Bone as a Function of Metaphyseal Location," J. Biomechanics, Vol. 16, No.12, pp. 965-969, 1983.
- 30. J.L. Lewis, M.J. Askew, and D.P. Jaycox, "A Comparative Evaluation of Tibial Component Designs of Total Knee Prostheses," *J. of Bone and Joint Surgery*, Vol. 64-A, No. 1, pp. 129-135, 1982.
- 31. M.H. Pope and J.O. Outwater, "Mechanical Properties of Bone as a Function of

- Position and Orientation, " J. Biomechanics, Vol. 7, pp. 61-66, 1974.
- 32. R.H. Macneal, *Nastran Theoretical Manual* Structural Modelling, The MacNeal-Schwendler corporation, Los Angeles, pp. 1.13-1 to 1.13-8 & 2.4-250 to 2.4-252, 1972.
- 33. G.A. Ateshian, L.J. Soslowsky, and V.C. Mow, "Quantitation of Articular Surface Topography and Cartilage Thichness in Knee Joints Using Stereophotogrammetry," *J. Biomechanics*, Vol. 24, pp. 761-776, 1991.
- 34. D.R. Carter, and W.C. Hayes, "Bone Compressive Strength: The Influence of Density and Strain Rate," *Science*, Vol. 194, pp. 1174-1176, 1976.
- 35. J.L. Williams and J.L. Lewis, "Properties and an Anisotropic Model of Cancellous Bone from the Proximal Tibial Epiphysis," *Trans. ASME*, Vol. 104., pp. 50-56, 1982.
- 36. R.B. Little, H.W. Wevers, D. Siu, T.D.V. Cooke, "A Three-Dimensional Finite Element Analysis of the Upper Tibia," *J. Biomechanical Engineering*, Vol. 108, pp. 111-119, 1986.
- 37. W.C Van Buskirk, and R.B. Ashman, "The Elastic Moduli of bone, in mechanical properties of bone," proceedings of the joint ASME-ASCE applied mechanics, Fluids Engineering and bioengineering conference AMD, Vol. 45, pp. 131-143, 1981.
- 38. J.E. Shigley and L.D. Mitchell, *Mechanical Engineering Design*, 3th ed., McGraw Hill, New York, pp. 63-65 & 245-247, 1977.
- 39. A. Shirazi-Adl, M. Dammak, A. Forcione, and G. Paiement, "Friction Measurements at the Bone-Implant Interface- Application to the Analysis of Cementless Prostheses," 38th Trans. Orthopaedic Research Society, pp. 382, 1992.
- 40. D. Rancourt, A. Shir; 7'-Adl and G. Drouin, "Friction Properties of the Interface Between Porous-Surfaced Metals and Tibial Cancellous Bone," *J. Biomedical Materials Research*, Vol. 24, pp. 1503-1519, 1990.
- 41. W.C. McCrone, R.G. Draftz, and J.G. Delly, *The Particle Atlas:* A Photomicrographic Reference for the Microscopical Identification of Particulate Substances, Ann Arbor Science Publishers, pp. 3-19, 1967.

- 42. R.M. Pilliar, J.M. Lee, and C. Maniatopoulos, "Observations on the Effect of Movement on Bone Ingrowth into Porous-surfaced Implants," *Clinical Orthopaedics & Related Research*, Vol. 208, pp. 108-113, 1986.
- 43. W.C. Hayes, L.W. Swenson, and D. Schurman, Axisymmetric Finite Element Analysis of the Lateral Tibia Plateau, J. Biomechanics, Vol. 11, pp. 21-33, 1978.